




Lateral flow biosensors based on the use of micro- and nanomaterials: a review on recent developments

Yan Huang^{1,2,3} · Tailin Xu¹ · Wenqian Wang¹ · Yongqiang Wen¹ · Kun Li² · Lisheng Qian² · Xueji Zhang^{1,2,4} · Guodong Liu^{2,3} 

Received: 3 May 2019 / Accepted: 12 September 2019 / Published online: 18 December 2019
© Springer-Verlag GmbH Austria, part of Springer Nature 2019

Abstract

This review (with 187 refs.) summarizes the progress that has been made in the design of lateral flow biosensors (LFBs) based on the use of micro- and nano-materials. Following a short introduction into the field, a first section covers features related to the design of LFBs, with subsections on strip-based, cotton thread-based and vertical flow- and syringe-based LFBs. The next chapter summarizes methods for sample pretreatment, from simple method to membrane-based methods, pretreatment by magnetic methods to device-integrated sample preparation. Advances in flow control are treated next, with subsections on cross-flow strategies, delayed and controlled release and various other strategies. Detection conditionst and mathematical modeling are briefly introduced in the following chapter. A further chapter covers methods for reliability improvement, for example by adding other validation lines or adopting different detection methods. Signal readouts are summarized next, with subsections on color-based, luminescent, smartphone-based and SERS-based methods. A concluding section summarizes the current status and addresses challenges in future perspectives.

Keywords Lateral flow assay · Strip biosensor · Vertical flow assay · Sample pretreatment · Flow control · Reliability improvement · Smartphone · Nanoparticles · SERS · Optical sensors

Introduction

The invention of lateral flow biosensors (LFBs) can track back to the early eighties of the last century [1]. Since then, LFBs have been used as commercial products for low-cost, simple-to-use, rapid tests for point-of-care screening of infectious diseases, drugs of abuse, and pregnancy [2]. However, there are long-standing criticisms of LFB as point-of-care tests (POCTs) and in field rapid diagnostic tests (RDTs), such as limited sensitivity, limited ability for quantification, inability for multistep performing and inability to multiplexing. Consequently, great efforts have been paid to improve the current situation of LFBs in recent years.

The retrospect of LFB's development reveals that LFB has attracted researchers' great attention in recent years, therefore loads of new ideas and researches have shot up then, leading to fruitful achievements and remarkable improvement on LFBs [3]. Since some nice reviews have summarized the development of label improvement [4, 5], quantitation [6] and multiplexing [7], in present paper, we focus on the aspects on

-
- ✉ Lisheng Qian
qianls@ahstu.edu.cn
 - ✉ Xueji Zhang
zhangxueji@szu.edu.cn
 - ✉ Guodong Liu
guodong.liu@ndsu.edu

- ¹ Research Center for Bioengineering and Sensing Technology, University of Science & Technology Beijing, Beijing 100083, People's Republic of China
- ² Institute of Biomedical and Health, School of Life and Health Science, Anhui Science and Technology University, Fenyang, Anhui 233100, People's Republic of China
- ³ Department of Chemistry and biochemistry, North Dakota State University, Fargo, ND 58105, USA
- ⁴ School of Biomedical Engineering, Shenzhen University Healthy Science Center, Shenzhen, Guangdong 518060 People's Republic of China

LFB design, sample pretreatment, flow control, reliability improvement and new signal readouts.

Design formats

Strip-based formats

Lateral flow strip biosensor (LFSB) is the most commonly used LFB, in which sample pad, conjugate pad, nitrocellulose membrane and absorption pad are laminated on a common sheet of plastic adhesive backing (Fig. 1a) [8]. LFSB has been dominating the POCT market because of the relatively slow commercialization of the POCT concept [9]. Generally, there are three binding systems employed in designing a LFSB, named antibody-antigen, aptamer-analyte, and DNA-DNA (or microRNA). When an assay starts, sample liquids containing targets are added to the sample pad and will flow towards absorbent pad due to the capillary force. Secondly, the target proteins or DNAs bound to the signal reporter-labeled detection antibodies or probes pre-coated on the conjugate pad. Thirdly, the formed conjugates flowed along the strip and

captured by the capture antibodies or probes immobilized on the detection area. Lastly, the captured labels in the detection area is measured by a transducer. The competitive assay and sandwich-type assay are the two most frequently used ones among the prevailing strip biosensors [10]. The competitive pattern is employed when the target analyte is with low molecular weight or presenting a single specific antibody. Nevertheless, in case that the target analyte owns more than one specific antibodies or DNA aptamers, sandwich-type pattern is more preferable [11–18].

Based on the above mentioned binding systems and design models, various LFSBs with different nanoparticle labels have been developed to detect DNAs, proteins [19, 20], bacteria cells [21, 22], virus [23], toxin [24, 25], inorganic ion (heavy metal ion) [26] and other chemicals [27]. One significant study described an gold nanoparticle (GNP) based LFSB for DNA detection. The detection process took 15 min with a linear range of 1–100 nM and a detection limit (LOD) of 0.5 nM. The LOD was improved to 50 pM by using horseradish peroxidase-coated GNP label, which catalyze enzymatic substrate to produce a colored product in the test area of LFSB (Fig. 1b) [28]. By combing the high

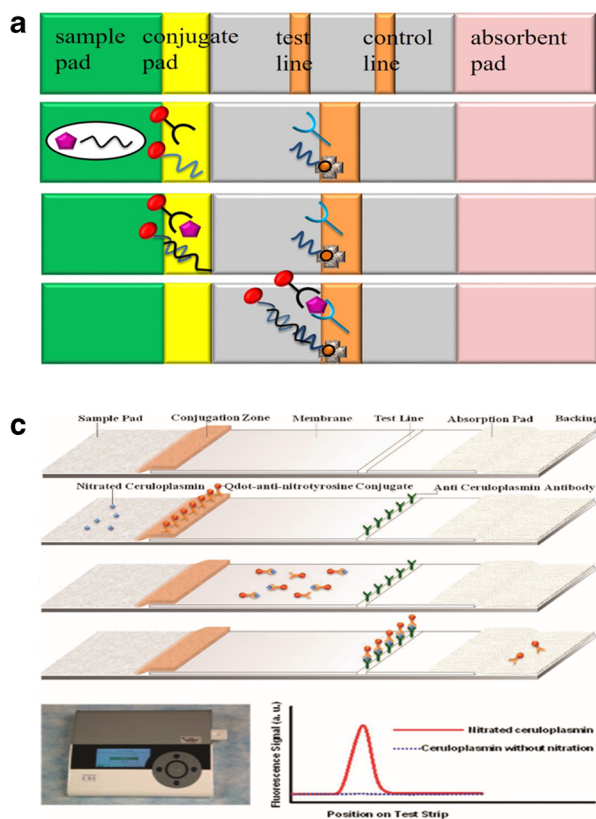
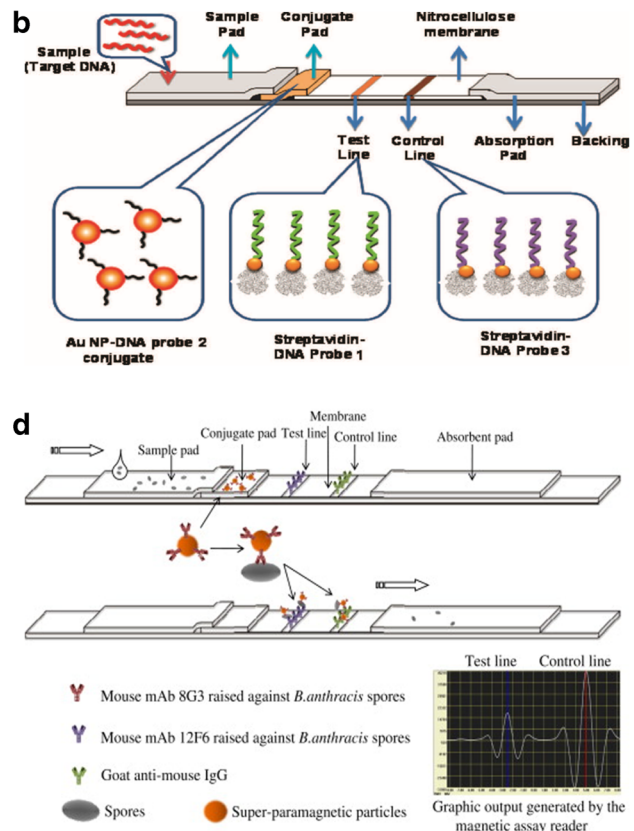


Fig. 1 a General schemes of LFBs with strip-based format. b GNP-based LFSB for DNA. Reproduce with permission from reference [28]. c QDs based LFSB for proteins. Reproduce with permission from reference [29].



d Magnetic nanoparticle-based LFSB for *Bacillus anthracis* spores. Reproduce with permission from reference [30]

photostability and superior signal brightness of quantum dots (QDs) with the convenience of LFSB, a QDs-based LFSB was reported for the detection of nitrated ceruloplasmin with an LOD of 1 ng mL^{-1} in buffer and 8 ng mL^{-1} in spiked human plasma sample (Fig. 1c) [29]. Superparamagnetic iron oxide particles were employed to design a portable super-paramagnetic LFSB for the detection of *Bacillus anthracis* spores. The system can detect 200 spores mg^{-1} in milk powder and 130 spores mg^{-1} in soil samples with a linear range of 4×10^3 – 10^6 CFU mL^{-1} (Fig. 1d) [30]. In another study, copper-dependent DNA-cleaving DNazyme was utilized to develop a LFSB for visual detection of Cu^{2+} . In the presence of Cu^{2+} , the DNazyme is cleaved at the special site and produces a specific DNA chain, which can be detected on the LFSB with an LOD of as low as 10 nM.

In summary, early LFBs with GNP label are used for qualitative (yes/no) or semi-quantitative assays. Emerging new nano-labels and sensitive transducers (color, fluorescent, magnetic, et al.) offer an avenue for quantitative detection. Most of strip-based LFBs contain a test line and control line, which are used to monitor the captured nanolabels. Because of the

limited area in strip-based LFBs, line-based multiplex assay on LFBs with high throughput will be difficult. Therefore, more efforts have to be put to develop LFBs with different designs for multiplex assay.

Cotton thread-based format

Since natural cotton threads are inexpensive, broadly available, light-weight, the cotton threads based devices owns unique advantages, such as low-cost, low-volume, easy-to-use, easily to handle after use, and multiplexing, which makes cotton threads promising support for transporting and mixing liquids. Cotton thread has been introduced as an alternative material for the assembling of LFBs [31–33].

Shen's group first fabricated thread-based and thread-paper-based 3D-structure LFBs for two important biomarkers, nitrite ion and uric acid. They demonstrate thread is a suitable material for the fabrication of lateral flow devices [31]. At the same time, Whitesides' group designed three cotton thread-based assays: "woven array", "branching design" and "sewn array". The thread-based devices can detect five different analytes (Fig. 2a). Thread was woven on a loom to enable multiple

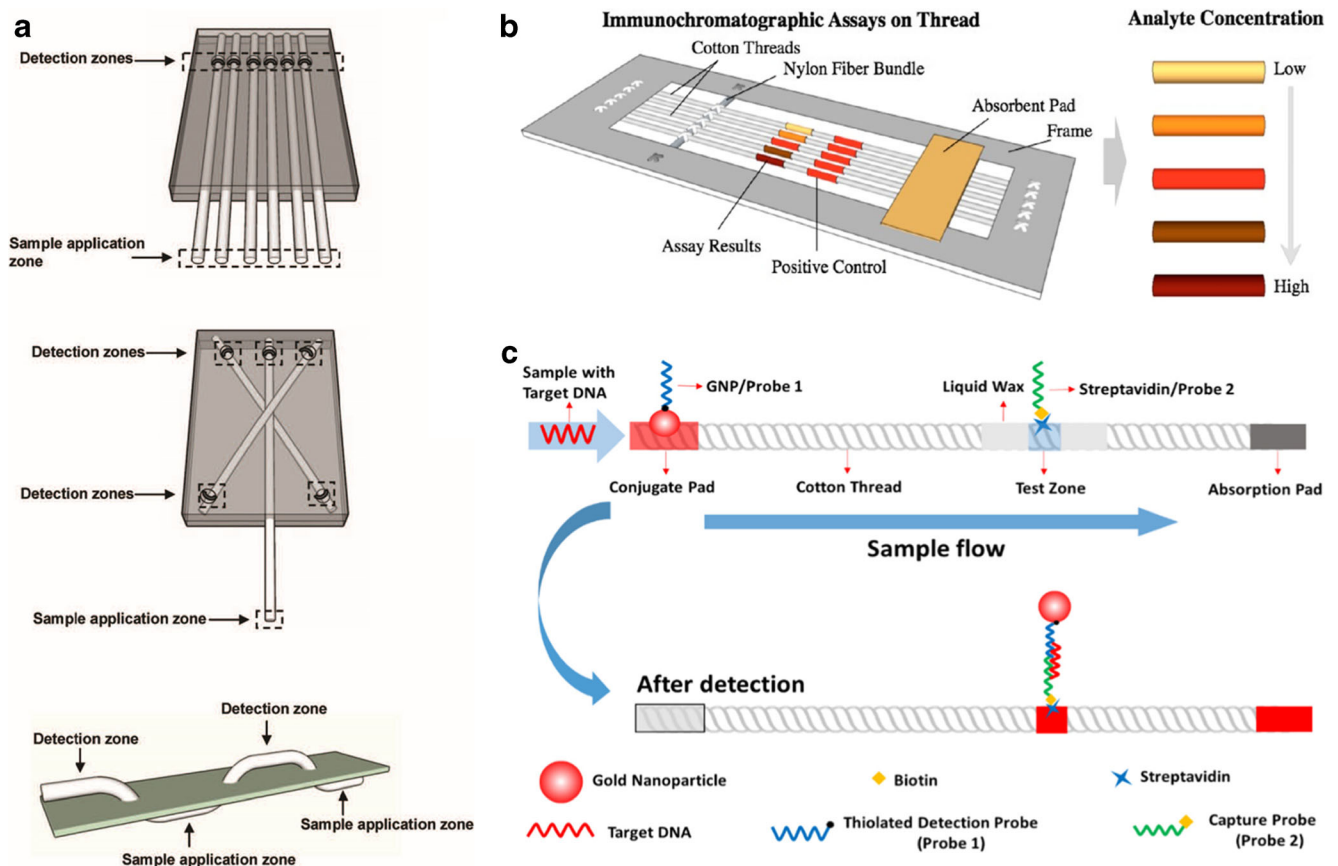


Fig. 2 a Schematic illustrations of thread-based devices including woven array device, the branching design and the sewn array design. Reproduce with permission from [32]. b Schematic illustrations of immunochromatographic assay for C-reactive protein. Reproduced with

permission from [34]. c Schematic illustration of the configuration and measurement principle of the temperature-dependent thread-based DNA biosensor and the test result at the presence of target DNA. Reproduce with permission from [39]

assays performing in parallel or sewn through a hydrophobic polymer sheet to incorporate assays into bandages-like systems, which demonstrated its ability of performing multiple assays in parallel [32]. Following their work, another study introduced the immunochromatographic assay on thread (ICAT) in a cartridge format which made it suitable for multiplexing (Fig. 2b) [34]. An LOD of 377 pM of C-reactive protein (CRP) was obtained. The possibility of multiplexing was demonstrated using three knotted threads coated with antibodies against CRP, osteopontin, and leptin proteins. After that, Mao et al. reported cotton thread based LFBs to detect DNA and proteins using GNP and nanocomposite labels. For example, they proposed dry-reagent cotton thread-based devices for the lung cancer related biomarker squamous cell carcinoma antigen (SCCA) and a human genetic disease, hereditary tyrosinemia type I related DNA sequences by using GNP labels [35]. One ng mL⁻¹ SCCA and 75 fmol DNA can be detected, respectively, in 20 min. By using GNP trimer reporter probe, the sensitivity on cotton thread was greatly improved and a minimum concentration of 10 ng mL⁻¹ human ferritin can be detected [36]. They also introduced carbon nanotubes (CNTs) [37] and carbon nanotube/gold nanoparticles (CNT/GNPs) nanocomposite [38] as labels on cotton thread-based assay, the LOD was 500 folds and 2–3 magnitudes improved respectively comparing with GNP or CNT as label. Figure 2c presents a cotton thread based biosensor for DNA with temperature-dependent pattern [39]. Liquid wax was placed to both sites of the cotton thread. This results in a concentration of the capture probe in this area after evaporation and translated into improved sensitivity.

Vertical flow- and syringe-based lateral flow biosensors (LFBs)

LFBs are originally defined to conduct along a single axis to fit the test strip format, nevertheless, can also be operated using vertical flow format. This alternative format of LFB, which called rapid vertical flow biosensors (VFBs), possess

several unique advantages including faster analysis time and the absence of hook effect. Like LFBs, VFBs are paper-based biosensors that use affinity chromatographic principle to separate targets from liquid sample and the assay chemistry is usually sandwich-type immunoassay. The key component of VFBs and LFBs is nitrocellulose (NC) membrane where capture antibody (cAb) is immobilized to capture the target. Membrane pore size and sample flow rate are two crucial factors to improve the sensitivity of VFB [40]. Newly interests came from its abilities to do multiplexed detection and handle large sample volume, with expectation that larger sample volume would lead to better sensitivity than LFB. Consequently, attention have been paid to explore VFB rather than LFB.

One study designed a VFB for C-reactive protein, with an analytical range from 0.01 to 10 µg mL⁻¹ within 2 min [41]. The VFB is simply assembled by stacking of all the components used in a lateral flow assay. The serum sample added to the sample injection hole can sequentially reach and wet the sample pad, conjugation pad, asymmetric membrane and NC membrane through the VFBs. Compared with the LFB system, the signal of the VFB increased gradually with the increase of target concentration without a hook effect. In Fig. 3a, the conventional lateral flow membranes were assembled in a stacking manner to prepare the VFB, where the liquid sample containing the analyte diffuses from the bottom to the uppermost layer to produce a colorimetric signal over an enzymatic reaction. *Escherichia coli* can be detected within 5 min with an LOD of 10² cells mL⁻¹, which is 1000 folds higher than that of ELISA [42]. In order to improve the sensitivity of VFB, another study successfully coupled VFB with surface-enhanced Raman scattering (SERS) for the determination of anti-HCV antibodies (Fig. 3b). The intense and highly reproducible SERS signals from the Raman reporters and the convenience of the VFB endowed this coupling system great potential for next-generation POC diagnostics [43].

Syringe, widely used in hospitals, factories and some research labs, can take in and expel liquid with easy pump operation. Syringe is an ideal candidate to construct VFBs.

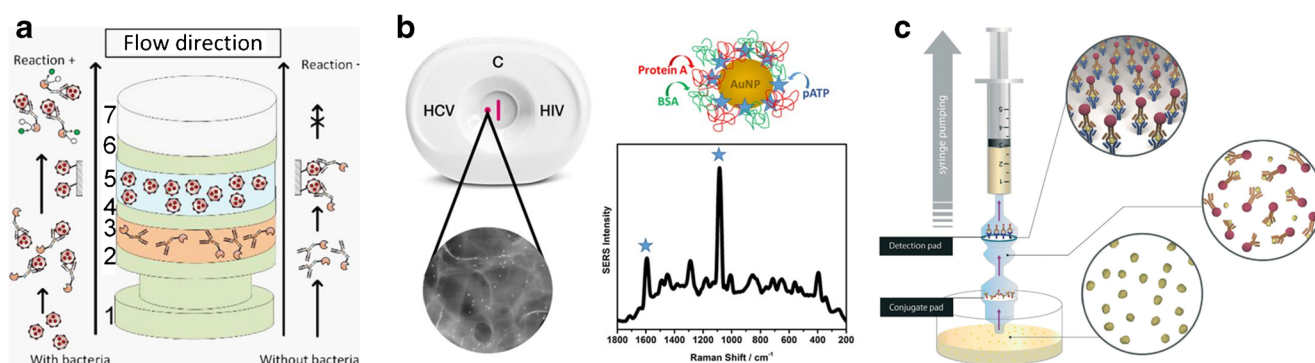


Fig. 3 **a** The structure of a typical vertical flow biosensor for *Escherichia coli*. Reproduce with permission from reference [42]. **b** VFA coupled with SERS for HCV antibody detection. Reproduced with permission

from reference [43]. **c** Working principle of the lab-on-a-syringe (LIS) based vertical flow biosensor for PSA. Reproduced with permission from reference [44]

A lab-in-a-syringe (LIS) featured simultaneous sampling and vertical-flow operation was developed for monitoring biomarkers. As shown in Fig. 3c, the LIS contains two nitrocellulose pads: the conjugate pad and the detection pad both embedded between reusable plastic filter holders connected to a reusable syringe. Owing the special ability of processing samples with large volume, the LIS design facilitates to preconcentrate the analyte, making it suitable for practical applications. The LOD was 1.0 ng mL^{-1} for human IgG and 1.9 ng mL^{-1} for prostate-specific antigen (PSA). In comparison with normal VFB, LIS can handle large-volume samples and thus get a better LOD [44]. In a similar work, a LIS device was designed for the colorimetric discrimination of alanine enantiomers. The LOD is determined as 0.77 mM in less than 5 min [45]. In another work, silver enhanced VFB for determination of oxytetracycline residues in fish tissues was described. The LOD was 2 ng mL^{-1} representing a 125-fold increase in sensitivity over the HRP labeled VFB [46].

Following their work, electrochemical [47] and thermochemiluminescence signals [48], as well as recombinase polymerase amplification, microarray based [49] and mobile phoned based [48] technology has been introduced to VFB to detect potential threats to national security and public health, such as pathogens, virus, and toxins.

For example, sandwich-type immunoreactions on the gold paper electrode of the immunostrip was performed in VFB to detect influenza virus. The electrochemical and colorimetric signals can reduce false results with double assurance [47]. Another work reported a multiplexed VFB for antibody assays in human sera. The results were imaged by a cost-effective mobile-phone reader and were sent to a server, where the results are rapidly analyzed and relayed back to the user [50]. Interestingly, a syringed-based VFB was developed by using syringe pressure readout to take place of color results. The principle was that Pt-nanoflowers behaved like catalase mimics to catalyze the decomposition of hydrogen peroxide to generate O_2 [51]. Works related to vertical flow assays and syringe-based biosensor are summarized in Table 1.

Sample pretreatment

Body fluids samples such as blood and saliva drops are most common sample matrix for disease diagnosis. Electrical and optical signals from the transducers are interfered by body fluids because the fluids are complex mixture of proteins, glucose, mineral ions and other substances [52, 53]. To improve the analytical performances of tests, body fluids can be

Table 1 Vertical flow assays and syringe-based lateral flow biosensors

Tracer	Analyte(s)	Detection mode	Detection method	Analytical sensitivities	Detection time	Syringe or not?	Ref.
GNPs	C-reactive protein	Antigen-antibody	Colorimetric	0.01 to 10 mg mL^{-1}	Within 2 min	N	[41]
GNPs	Prostate-specific antigen	Antigen-antibody	Colorimetric	1.9 ng mL^{-1}	Within 10 min	Y	[44]
Flucytosine	Flucytosine	Direct detection	SERS	$10 \text{ } \mu\text{g mL}^{-1}$	15 min	N	[59]
GNPs	L-Alanine	enantioselective interaction	Colorimetric	0.77 mM	Within 5 min	Y	[45]
GNPs	<i>Escherichia coli</i>	Antigen-antibody interactions	Colorimetric	$10^2 \text{ cells mL}^{-1}$	Within 5 min	N	[42]
Reporter-modified GNPs	Anti-HCV antibodies	Antigen-antibody interactions	Colorimetric/SERS	1/1024 diluted antibody	Not reported	N	[43]
Horseradish peroxidase	Influenza H1N1 viruses	Antigen-antibody interactions	Electrochemical/colorimetric	3.3 and 2.27 PFU mL^{-1} by EIS and colorimetric	6 min	N	[47]
GNPs	<i>Burkholderia pseudomallei</i>	Antigen-antibody interactions	Colorimetric	0.02 ng mL^{-1}	Within 30 min	Y	[40]
GNPs	<i>Borrelia burgdorferi</i> antigens	Antigen-antibody interactions	Colorimetric	209.6 ng mL^{-1}	20 min	N	[50]
GNPs	Oxytetracycline residue	Antigen-antibody interactions	Colorimetric	2 ng mL^{-1}	Within 4 min	N	[46]
GNPs	Adenoviralt	Nucleic acid hybridization	Colorimetric	50 nM	Not reported	Y	[49]
Reporter modified silica	Valproic acid	Antigen-antibody interactions	Thermochemi-luminescence	4 in blood and $0.05 \text{ } \mu\text{g mL}^{-1}$ in saliva	In 12 min	N	[48]
Pt-nanoflowers	Pathogenic bacteria	catalyze H_2O_2 to generate O	Optical	15 and $7 \text{ CFU}\cdot\text{mL}^{-1}$	Not reported	Y	[51]

pre-handled to get rid of interfering components. The fluids can be diluted to suit the dynamic range of a certain examine, or concentrated to enrich the amount of a particular analyte within a given volume of sample. Therefore, LFBs integrated with sample pretreatment would have a great significance for realizing detection in real sample and distinctly improve the accuracy and LOD. According to Niedbala et al., the common used methods for pretreatment of sample solution in a lab included sample dilution, centrifugation, immunoglobulin removal, centrifugal filtration with different molecular weight cut off and filtration through active adsorbent materials [54]. However, these methods are not suitable for certain situation, for example, sample dilution reduced the interference while at the cost of diminishing the sensitivity; centrifugal filtration can effectively eliminate the interference, but was intrinsically impractical for POCT. The following sections will highlight such sample pretreatment integrated LFBs.

Simple sample pretreatment

Oral fluid is a complex mixture of proteins, mucus, and other substances that can induce the aggregation of reporter gold particles. A simple filtration strategy was introduced into LFB for the cotinine nicotine metabolites in oral fluids. To overcome this aggregation and enable filtration to minimize the interferant effect without high pressure, Nylon filters with 0.45 μm pore size was used. With simple filtration strategy sample pretreatment, 2 ng mL^{-1} of cotinine nicotine metabolites in oral fluids can be detected within 15 min [54]. An

integrated paper-based cadmium (Cd^{2+}) immunosensing system is shown in Fig. 4a. The systems integrated a sample treatment process, which is an added conjugation pad providing Cd^{2+} complexation with EDTA and interference masking through ovalbumin (OVA). Important potential interferences such as Mg^{2+} , Cu^{2+} and Zn^{2+} were greatly reduced or completely removed employing OVA. The detection and quantification limits were 0.1 and 0.4 ppb, respectively, holding the lowest detection limits for metal sensors based on paper [55]. In another work, a method of sampling and evaluating wound biomarkers was demonstrated for clinical applications using a thermally reversible hydrogel. The thermally reversible hydrogel sampled and insulated biomarkers within a wound surrounding. Then such thermally reversible hydrogel was investigated in the LFB employing fluorescent microspheres as label without further sample extraction/pretreatment steps. The LOD for chronic wound biomarkers interleukin 6 and tumour necrosis factor alpha are 48.5 pg mL^{-1} and 55.5 pg mL^{-1} respectively in hydrogel samples and 7.15 pg mL^{-1} and 10.7 pg mL^{-1} respectively in plasma [56].

Sample pretreatment by membrane-based methods

As chromatography is originally a separation technique, sample pretreatment can be achieved on the membrane-based strips. In one study, a lateral-flow based method was clarified and characterized for gathering the target DNA concentration from lysed blood. The capture sequence, which is complementary to the target sequence, was cross-linked on the nitrocellulose by

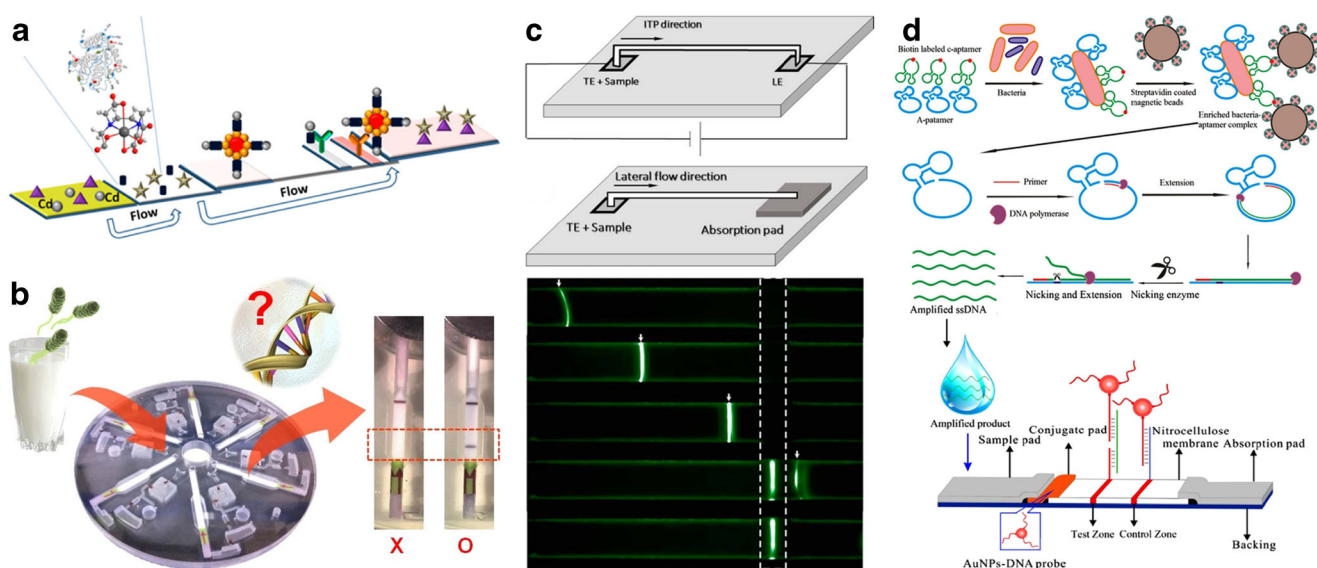


Fig. 4 LFBs with sample pretreatments. **a** Sample pretreatment with additional conjugate pad for cadmium. Reproduce with permission from reference [55]. **b** Device integrated sample preparation and for *Salmonella* detection. Reproduce with permission from reference [71]. **c**

Sample pretreatment using ITP-based chromatography for DNA. Reproduce with permission from reference [61]. **d** Sample pretreatment using magnetic separation for *Salmonella enteritidis*. Reproduce with permission from reference [63]

exposing to a UV light. After the target DNA was captured and washed, the capture region was excised and denatured in sodium hydroxide. The resulted eluate, with 7 times tolerance ability enhancement for interference, can be used for RPA amplification or detected on a LFB [57]. In another study, a glass fiber, semi-permeable membrane and PEG solution were employed to design the membrane-based dialysis concentration device. PEG was chosen as a dialysate by virtue of its good hygroscopic property to facilitate the small molecules to cross the selective semi-permeable membrane. After dialysis 10 min, the concentrated sample was applied to the LFB. Using the sample concentration device, a 10-fold signal enhancement in Human Immunodeficiency Virus (HIV) nucleic acid detection and a 4-fold signal enhancement in myoglobin (MYO) detection was achieved, respectively [58]. In the third study, nitrocellulose membranes in the vertical-flow format as the filtering membrane to separate 5-fluorocytosine (5FC) from serum. The membrane can selectively trap serum components while transporting the target 5FC. The 5FC was then absorbed on the nanoparticle of an inkjet-fabricated paper SERS sensor beneath the filtering membrane and detected with a portable Raman spectrometer [59]. Electrokinetic preconcentration and separation technique named isotachopheresis (ITP) were employed onto LFB aiming at improving its LOD. Such ITP on nitrocellulose is capable of up to a 900 fold increase in initial sample concentration and up to 60% extraction from 100 μL samples and more than 80% extraction from smaller sample volumes [60]. Following this experiment, they gathered target analytes into a narrow band and then conveyed them to the LFB capture line, bringing about an impressive increase in the surface reaction rate and equilibrium binding (Fig. 4c). They manifested that ITP is able to promote the LOD by 400-fold for 90 s assay time. The ITP-enhanced LFB also shows equivalent to 30% target extraction from 100 μL sample liquid, whereas conventional LFB gains less than 1% of the target [61].

Sample pretreatment by magnetic separation and magnetic focus

Taking advantage of supermagnetism, magnetic beads-based separation is a convenient way to perform sample pretreatment. For example, silica-coated magnetic nanoparticles were used to separate nucleic acid from *Cronobacter* lysate and eliminate the interference of food matrices in a LFB. The detection limit was 10^7 cfu mL^{-1} in pure culture without any other pretreatment. After pretreatment with silica-coated magnetic nanoparticles, the detection limit was 10^5 cfu mL^{-1} in pure culture and maintained stable even under the interference of 10^8 cfu mL^{-1} *Salmonella typhimurium* [62]. Following the same principle, an aptamer-based biosensor was reported for rapid detection of *Salmonella enteritidis* (*S. enteritidis*) (Fig. 4d). One of the

aptamers specific for the outmembrane of *S. enteritidis* was linked to streptavidin coated magnetic beads and used for magnetic bead enrichments. Another aptamer against *S. enteritidis* was used as a reporter for this pathogen, which was amplified by isothermal strand displacement amplification (SDA) and further detected by a lateral flow biosensor [63]. Likewise, super-paramagnetic particles labeled with antibodies was used to enrich *Bacillus anthracis* spores from sample. The magnetic particles-spores complex were re-suspended in running buffer and detected on a LFB. Such magnetic particle was used as both separation and the color label. Without any other sample pre-treatment, they realized *Bacillus anthracis* spores detection in 25% (w/v) milk, 10% (w/v) baking soda and 10% (w/v) starch [64]. Based on the same magnetic enrich methods, multiplex detection of nitro-furan metabolites was realized without tedious organic reagent-based extraction procedure [65]. Importantly, sample-processing steps was added to the front of the commercial diagnostic process. The protein biomarker from blood was purified by proceeding biomarker bound magnetic particles through a low-resource extraction cassette employing a hand-held magnet. Five commercial rapid diagnostic tests brands were enhanced for 4 to 13 folds after sample processing [66]. In another work, Fe_3O_4 nanoparticles were coated on the CNT surface to prepare magnetized carbon nanotube (MCNT). Proteins can be recognized and separated by the MNCT-antibody conjugates from the blood, and then be detected on the LFB. Rabbit IgG [67] and carbohydrate antigen 19-9 [68] were detected in blood with a detection limit of 10 ng mL^{-1} and $30\text{ U}\cdot\text{mL}^{-1}$, respectively. Instead of put the magnet outside a centrifuge tube, a magnet was put beneath the sample zone of the LFB for extraction magnetic nanoparticle-Ab-analytes from matrices solution. The distance between the strip and the magnet was the key to adjust the strength of the applied magnetic field. On the one hand, the beads can be extensive penetrated into the NC membrane and not be able to release upon removal of magnet, when the magnetic field is too strong. On the other hand, almost all the beads would flow through the sample zone when the magnetic field is too weak [69]. Compared to the magnet was put beneath the sample zone in the above work, the magnet was placed beneath the detection zone of LFB for the purpose of increasing interaction time between the magnetic probe-labeled targets and the capture antibody, which delivered a 106-fold improvement in sensitivity compared to that of conventional LFB [70].

Device-integrated sample preparation and detection

Integrating the sample preparation and detection into one device reduces the size of the device, minimizes the operation procedure and shortens the detection time, which have great significance in resource-limited areas. Kim et al. reported a

fully integrated lab-on-a-disc for nucleic acid analysis of foodborne pathogens (Fig. 4b). The cell in PBS and milk samples were first magnetically separated. The following DNA extraction, amplification, and lateral flow assay were integrated into a disk. Valve actuation, cell lysis, DNA extraction and amplification were all controlled by a single laser diode, making the system compact and miniaturized [71]. Inspired by this study, the lab-on-a-disc was used to detect pathogen. Instead of using a laser diode, the fluidic was controlled by coriolis force and siphon valving structures, thus making both singleplex and multiplex for pathogen available. In another work, DNA from the lysate sample was extracted using a glass microbead strategy, which facilitate the final detection on LFBs [72]. Likewise, nucleic acid extraction, amplification and visual detection or quantification using a smartphone were integrated into a paper-based biosensor with 4 layers, the top PVC layer of the conventional LFB, the second layer of a glass fiber for nucleic acid amplification procedure, the third layer of a Fast Technology Analysis card for sample application and nucleic acid extraction, and the bottom layer of an absorbent pad for sample purification and washing. With such integrated biosensor, *Escherichia coli* in spiked drinking water, milk, blood, and spinach and *Streptococcus pneumonia* in clinical blood samples were successfully detected in 1 h [73].

Flow control

Though LFBs fulfill many of the ASSURED criteria, they have been criticized for both their inability to multiplex (i.e., assay for multiple analytes from a single sample) and their inability to perform multistep chemical processing with a resultant poor sensitivity for many analytes of clinical importance [74]. The development of a new LFB design that incorporates a fluid control mechanism may be a way to solve the problems. There are several advantages with the ability to control fluid flow, including the following: (1) more complex and intricate assays can be developed; (2) subsequent loading of buffers and solutions can be allowed; (3) the waiting time for loading after incubation can be eliminated; (4) the amount of labor used for performing an assay can be reduced. Therefore, user error can be effectively reduced. Flow control is of great value not only in the biomedical, food and environmental fields, but also in diseases diagnosis in low resource settings.

Cross-flow strategy

Applying a subsequent color substrate after the immunoreaction is a normal way for both color signal production and signal enhancement. While the water capacity of the absorption pad is limited, adding solutions to flow across the width of the test area of the strip would be a better solution, which

is the so-called cross-flow strategy. For example, a cross-flow POCT biosensor was reported for cardiac troponin I (cTnI) by incorporating a vertical flow to the conventional LFB. Sample containing cTnI was first applied on the LFB. After 15 min the substrate solution for HRP was added to the membrane, which is partial superimposition and perpendicular to the test area of former membrane strip, to generate a color signal. In this way, antigen-antibody bindings and catalytic reactions were sequentially accomplished through cross-flow chromatography in the vertical and horizontal directions respectively [75]. Using the same cross-flow strategy, immunogold–silver staining adopted to enhance the signal intensity of a traditional LFB for cTnI was reported (Fig. 5a). Compared with the conventional incubation mode by immersing the membranes in the bulk solution, the cross-flow silver staining procedure made POCT available with the silver intensification. The sensitivity was enhanced by 51-fold compared to the traditional GNP-based LFB [76]. In another work, by introducing the cross-flow strategy, the non-specific interaction between the GNP and the membrane surface caused by the physical properties change of the GNP at a high concentration can be overcome [77]. The operation procedure of cross-flow strategy was minimized by integrated the LFB into a two-dimensional paper network card. Twenty minutes after the detection of human chorionic gonadotropin on a commercial strip, the subsequent rinse and amplification steps were initiated by simply closing the two dimensional card, by which a 4-fold signal enhancement was achieved [78]. The cross-flow idea was extended for sequential delivery of more than two reagents to a test strip. A rotary device consisting of two portions that can rotate with each other was demonstrated in Fig. 5b. Compared to the previous methods that require manual rearrangement of pads, incremental rotation by a simple hand motion can change the connected pads preloading with different reagents to the test strip and facilitate sequential delivery of multiple reagents. An operation of strip-based ELISA for simple colorimetric detection of *E. coli* O157:H7 was demonstrated with the device [79].

Delayed release

Delayed release strategy can be used in LFBs to enable automatic implementation of multiple steps and realize target detection with a single sample solution. For example, an asymmetric polysulfone membrane (ASPM) used to realize the delayed-release effect of chemiluminescence substrates is demonstrated in Fig. 5c. ASPM was placed between the nitrocellulose membrane and the substrate pad. The pore sizes in the ASPM gradually increases from the side connected to the nitrocellulose membrane to the other side in contact with the substrate pad. By virtue of that it is unfavorable for the solution to flow from the smaller pore to the larger pore,

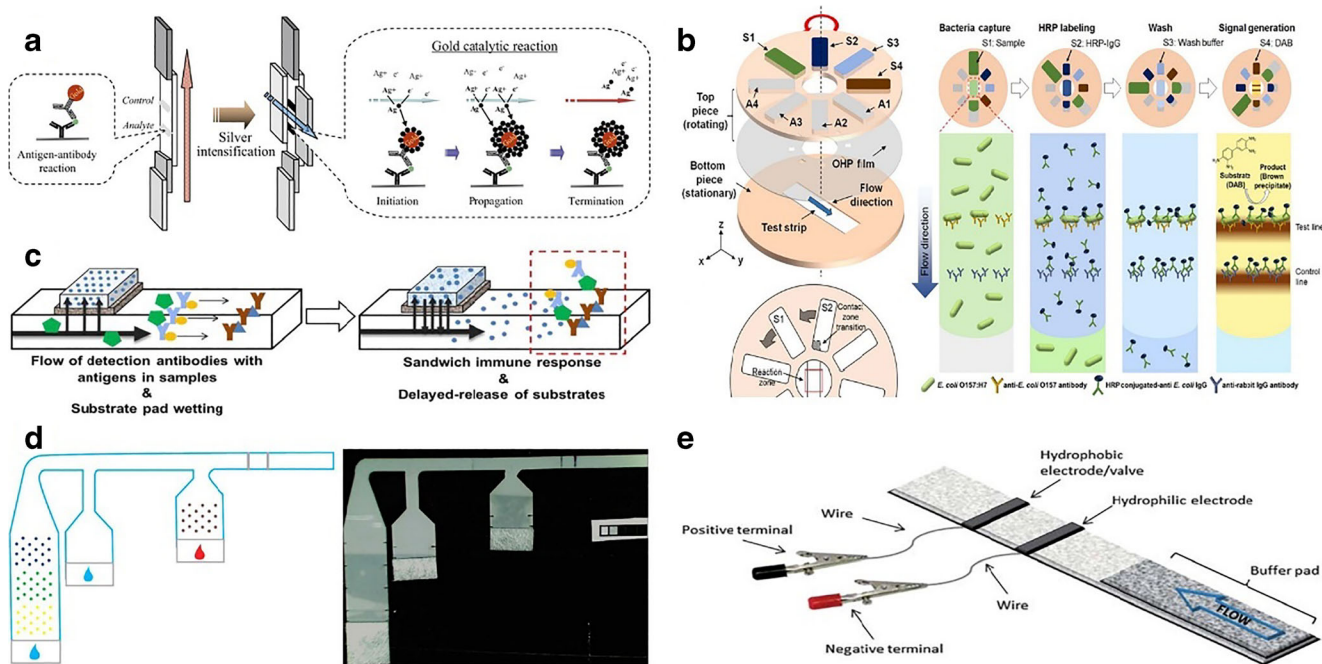


Fig. 5 **a** LFB based on sequential cross flow for cardiac troponin I. Reproduce with permission from reference [76]. **b** LFB based on multiple reagent delivery for *E. coli* O157:H7. Reproduce with permission from reference [79]. **c** LFB with delayed release strategy for C-reactive protein. Reproduce with permission from reference [80]. **d**

LFB with controlled release strategy for *Plasmodium falciparum* histidine-rich protein 2 detection. Reproduce with permission from reference [88]. **e** LFB with a hydrophobic and a hydrophilic electrode for *Saccharomyces cerevisiae* rRNA sequences. Reproduce with permission from reference [89]

the ASPM was wetted slowly during the assay. As a result, the substrates wrapped in the substrate pad were released 5.3 ± 0.3 min after the detection started. Using this delayed-release effect, immunoreaction, pH change, substrate release, hydrogen peroxide generation, and chemiluminescent reaction was sequentially performed with one simple sample application on the designed chemiluminescence LFB [80] or electrochemical LFB [81]. Instead of using ASPM in the above work, delay release of the second reagent can also be realized using a water-swellaible polymer. Upon the application of the sample solution, the immunoreaction took place like that on the conventional LFB. At the same time, the solution was absorbed to the second reagent pad vertically above the NC membrane, soaked the pad and the water-swellaible polymer under the pad. The expansion of the water-swellaible polymer resulted in the attachment of the reagent pad and the NC membrane, and then the release of the second reagent [82]. In another study, the core-shell hybrid nanofibers were deposited by coaxial electrospinning method in front of the test line on the NC membrane of the LFB. The water-soluble polymer in the shell of the hybrid nanofibers would dissolve after the occurrence of the antibody-antigen reaction and release silver reducing reagents in the core. The LOD of a commercial LFIA was enhanced up to 10 times [83]. A trapezoid shape of sample pad was designed by wax-printing to facilitate the solution flow and improve the sensitivity of assay. The color substrate

in the wax-delayed channel can be delayed for 11 s to move to the test line and export the color signal [84].

Controlled release

To improve the appropriateness for POCT, one should minimize the operation steps. A prototype was demonstrated with 3 inlet to perform signal enhancement processes on paper networks. Reagents were dropped to the 3 inlet simultaneously and reached at the detection area sequentially due to different distances between detection area and the inlet [85]. Following this work, the same group designed a two-dimensional paper network card to minimize the operation procedure for users in low-resource settings. The 3-inlet reaction system can be initiated by simply closing the card [86]. By encircling the reagent spot with sugar barrier, Fridley et al. adopted the delayed rehydration strategy of printed reagents and demonstrated 4.1 (± 0.2) fold gold signal enhancement system by one-step application of solution. Sugars in the reagent solution can increase the viscosity of the rehydrated reagent solution and provide control over the dissolution time of reagents dried in polydimethylsiloxane [87]. Combining the above two work, a LFB with 3 inlet and four patterned separate reagents was designed (Fig. 5d). The LFB performed both target detection and signal enhancement on a one-step solution application. The signal enhancement by the controlled rehydration from patterned reagent storage depots was demonstrated to be 3-fold [88].

Other flow control strategy

In order to improve the LFBs ability in controlling the rate of fluid flow during an assay, there are several other interesting and creative works. Paper-fluidic devices with conductive hydrophilic electrodes and hydrophobic electrodes/valves are demonstrated in Fig. 5e. The hydrophobic electrodes/valves can block the fluid at front of the detection line, while an applied potential can transform the fluorinated monolayer on the electrode and actuate the hydrophobic valve. The amount of time for the fluid to pass the valve would decrease with the increase of the applied potential between the electrodes due to the rapid alternation of the monolayer [89]. Flow control can be realized from the area of device facet by devising a sliding strip allowing a central patterned paper strip to slide in and out of fluidic path. The linear motion of the sliding strip acted as a valve to control the serial introduction of sample, wash buffer, amplification reagents and reagents [90]. In another work, centrifugation-assisted LFB was proposed by preparing a vaulted piece of NC membrane and putting it into a centrifugal disc for the purpose of enhancing sensitivity. Under the optimized rotation speeds and sample volumes, the sensitivity of PSA was improved 6.2-fold compared to that of ordinary LFB [91].

Several exquisite works pointed at increasing the reaction time on the test zone by decreasing the flow rate. A flow delay strategy was developed by integrating a glass fiber shunt and a hydrophobic polydimethylsiloxane (PDMS) barrier into the LFB for sensitivity enhancement on DNA. By reducing the fluid wicking rate, the shunt increased the reaction time of GNP-probe and target before being capture by streptavidin on the test area. The PDMS barrier was used as an obstacle to delay the sample flow for further sensitivity enhancement. After optimization of the length of the shunt and the drops of the PDMS barrier, a 10-fold signal enhancement was achieved compared to conventional unmodified LFB [92]. The flow rate was reduced in another work by hydrophobic coating of polycaprolactone (PCL) onto NC membrane with electrospinning technology. The sensitivity of nucleic acid assays was increased for approximately ten-fold compared to the unmodified LFB [93].

Improvement of reliability

The reliability (or accuracy) is a generally verified challenge for RDT [94, 95]. There are two accepted approaches to improve the detection accuracy in order to avoid false results. One way is to insert another “validation line” as a supplementary for testing. The other way is introducing a different detection approach to double confirm the detecting result.

Adding another “validation line”

In order to overcome the obstacles that LFBs often have the limited ability in measuring an expansive concentration range of target by cause of the “hook effect”, an extra antigen line between the test and control lines was introduced to the LFB (Fig. 6a) [94]. They chose C-reactive protein (CRP) as a proof of concept. Different color changes were observed on the three lines. The color intensity of the test line increased from 0 to $1 \mu\text{g mL}^{-1}$ but decreased at higher CRP concentration because of the hook effect. The signal intensity of the antigen line showed a gradual decrease along with the CRP concentration increasing due to the decreasing of the free antibody-GNPs. The control line displayed the highest signal at high CRP concentration by virtue of binding with the most unreacted GNP-conjugate-antigen complex resulting from the minimum total GNPs capturing on the test and antigen line. After data processing the three lines, a wide linear detection range of $0.69 \text{ ng mL}^{-1} - 1.0 \text{ mg mL}^{-1}$ was obtained. Based on Y-shaped junction DNA and target recycling amplification, a three-line lateral flow biosensor for logic detection of microRNA was reported (Fig. 6b). In the presence of the target miRNA, a Y-shaped junction structure formed and one chain of the Y-shaped DNA was cleaved by an endonuclease to produce two DNA fragments. At the same time, the regenerated two chains entered into the next cycle of the amplification. The accuracy was improved and false results were avoided by detecting two different DNAs on the LFB [96]. For the sake of avoiding the false negative results possibly caused by the failure of amplification, internal amplification control (IAC) line was added to the nucleic acid LFB for the detection of single-stranded PCR amplicons. Because the biosensor was designed to detect the PCR amplified product and any inhibition to the amplification progress will result in a false negative result, the IAC line was introduced to prove the occurrence and provide a validation for the amplification process [97]. Likewise, an IAC line was introduced to the LFB for quantifying virus loads in a blood sample. The IAC line was the internal quantification standard of a target and monitor the whole procedure including nucleic acid extraction, amplification, and detection [98].

Adopting different detection methods

Compared with tests based on a single detection method, the integration of two methods provided double confidence and can potentially avoid false results getting from one method. The measurement reliability can be greatly improved by combining LFBs with more accurate analytical methods such as the electrochemical, fluorescent, magnetic and SERS assay. Zhu et al. reported a paper electrode integrated LFB for quantitative analysis of oxidative stress induced DNA damage (Fig. 6c). The captured target on the test line was colorimetric measured and the captured target on the control line was simultaneously

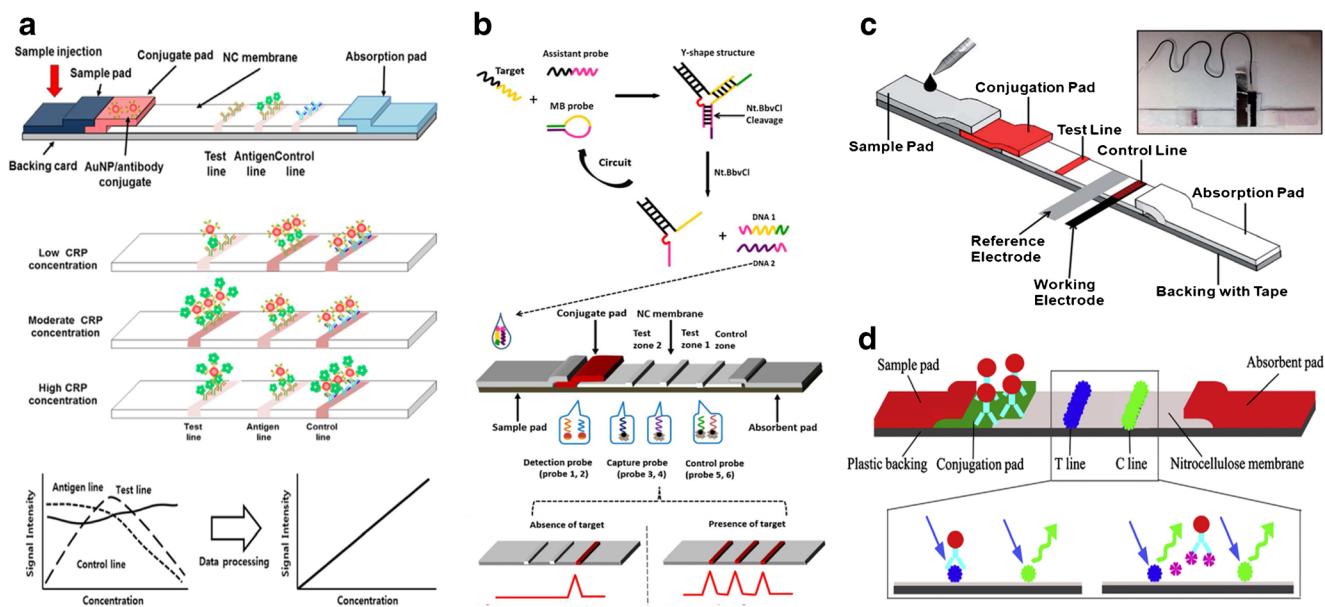


Fig. 6 **a** Three-line LFB with an extra antigen line for C-reactive protein. Reproduce with permission from reference [94]. **b** Three-line LFB with two detection lines for DNA detection. Reproduced with permission from reference [96]. **c** LFB based on both electrochemical and colorimetric

method for DNA oxidative damage biomarker detection. Reproduced with permission from reference [95]. **d** LFB based on both fluorescence and colorimetric method for Clenbuterol detection. Reproduced with permission from reference [99]

electrochemical determined [95]. In another study, dual-functional LFBs were applied for monitoring small molecule analytes based on the fluorescence-quenching effect of GNPs. Fluorescent signals were proportional to the target concentration generated under excitation light while colorimetric signals were inversely proportional to the target concentration under natural light. The sensitivity of the former is 125 folds better than that of the latter (Fig. 6d) [99]. In another work, one LFB was reported for *B. anthracis* spore. Instead of the conventionally reported test lines and control lines in a typical LFB, the principle relied on the fact that the complexes formed by *B. anthracis* spores, super-paramagnetic particles and antibodies were large enough to block the pores of chromatographic strips and consequently form a retention line. By interpreting signals from the retention line, optical, magnetic and visual determination can be simultaneously realized [64]. The SERS tags are often Raman reporter-labeled GNPs, consequently, colorimetric and SERS signals can be both obtained in a SERS based LFB. The colorimetric results were observed by bare eyes and the SERS spectra were acquired by a portable B&W Tek i-Raman Plus [100].

Effects of detection conditions and mathematical modelling

Apart from the mainstream studies of the LFBs, there are some researchers who focus on unusual but important aspects of LFBs such as the reaction temperature and humidity, the stability and storages and the development of the mathematical model.

Environmental factors including temperature and relative humidity (RH) has big influence on both nucleic acid hybridization and antigen–antibody interaction. One study investigated this issue with a portable temperature–humidity control device. The result showed the fluid was unable to completely diffuse across the nitrocellulose membrane at low humidity, whereas $RH > 60\%$ can effectively facilitate the fluid to completely wick through the paper. Signals of LFBs based on nucleic acid hybridization with a temperature of 55–60 °C and a humidity of 70–90% were enhanced 10 folds over ambient conditions (25 °C, 60% RH). At the same humidity, the sensitivity of LFBs based on antigen–antibody interaction with a temperature of 37–40 °C was improved 3 folds compared to ambient conditions [101]. Under extremely high temperature conditions, such as a delivery truck or train in summer, the stability of test strips decreases rapidly because antigens and antibodies in the strip are seriously influenced by high temperatures. To increase the stability of the LFB, the goat anti-mouse antibody immobilized on the NC membrane was mingled with three protecting agents, including WellChampion, antibody enhancer, and Protein stabilPLUS. Then the mixed solution was dispensed on the NC membrane and put in a drying oven at 60 °C for three weeks. Variations were checked employing negative and positive swine urine samples. The results revealed that WellChampion can efficiently enhance the stability of the LFB while the other two were not able to [102].

As the improvement of the LFB technology demands huge experimental works, computer simulations can be efficient tools to develop novel devices. The virtual experiments require less costs and time compared with real LFB prototypes.

One study described a mathematical model for an immunochromatographic serodiagnostic assay. By analyzing the model, the key factors of the assays were identified including the reagent concentration in the marker conjugate, the concentration in the test zone, the association and dissociation constants of the immune complexes and the serum dilution. From the calculations, using the highest possible concentrations of the reagent concentration in the marker conjugate and testing the serum dilutions from 10 to 100 times can improve the LOD of an immunochromatographic serodiagnostic assay [103]. In another work, a computational tool used for LFB was presented, including the fluid dynamics, reactive components transportation, and the biochemical reactions. Such computational tool is useful to explore arbitrary architectures, materials, and assay formats [104]. Likewise, a simple geometrical work was carried out to study the impact to the flow velocity and reaction rate kinetics by changing the pad width and test line position. Results showed that the pad with a narrow width and longer distance between the test line and conjugate pad contributed to color intensity for up to 400% of increase [105].

Signal readouts

Early LFBs with visual detection are used for qualitative (yes/no) or semi-quantitative analyses. Signal readouts based on color (camera installed strip reader), electrochemical signals (current), magnetic property, luminescent and Surface-Enhanced Raman Spectroscopy (SERS) have been integrated with LFBs for quantitation of the analytes. The use of signal readouts is based on the labels used in the lateral flow assay. The sensitivities of LFBs have been improved dramatically by using nanomaterial labels with unique optical properties. In this section, we focus on the optical signal readouts based on color, luminescent and SERS.

Color-based signal readouts

Among the commonly used micro/nano-particles on LFBs (Table 2), colloidal gold nanoparticle (GNP) is the most widely used. GNP can be easily conjugated with biomolecules, and the biochemical activity of the tagged biomolecules is still retained [106, 107]. GNP has been widely used as colored labels in LFBs due to their excellent surface effect and unique optical properties [2, 28, 108–110]. Several groups have successfully developed quantitative LFBs based on GNP labels and portable strip reader for nucleic acids [28, 111–115], microRNA [96, 116, 117], proteins [118, 119], cancer cells [109], and small molecules [120–123]. The strip reader consists of a digital camera, which take the images of the test line and control line, and a software. Based on the intensities of

test line, the strip reader can quantify the concentration of the analyte tested.

One example to detect ricin was based on the sandwich format with two monoclonal antibodies [124]. Besides antibodies, single strand DNA and aptamers have been used as recognition elements to conjugate with GNPs for the color-based LFBs. One work described a LFB with two DNA probes for DNA, the linear range of which is 1–100 nM with a LOD of 0.5 nM. The LOD was improved to 50 pM by using horseradish peroxidase coated GNP dual label [28]. Following this work, isothermal strand-displacement polymerase reaction (ISDPR) was employed to improve the sensitivity of the GNP-based LFB. Due to the great amplification ability of ISDPR, such system was 1000 times more sensitive than the above work [115]. A DNA-GNP based LFB was developed for visual detection of microRNA (miRNA)-215 in aqueous solutions and biological samples (Fig. 7a). A minimum concentration of 60 pM miRNA-215 was detected [116]. Another two works was conducted to improve the LFB's sensitivity. In the first work, HRP was immobilized on the GNP surface. Sensitivity was amplified for 10 times by applying the color substrate with a LOD of 7.5 pM [117]. Y-shaped junction DNA probe associated with endonuclease-assisted target recycling amplification were introduced to the second work. As low as 0.1 pM miRNA was visually detected in aqueous solutions, resulting in a 100–1000 times improvement of sensitivity [96].

Aptamers, the artificial functional oligonucleotides, own some distinct characteristics, such as the high association constant with target proteins and small molecules, readily to be labelled with signal moieties, easy to obtain, cost-effectiveness, and long-term stability. They have been exploited to incorporate with a diversity of small molecules, proteins and DNAs. One work introduced an aptamer to conjugate with GNP for the detection of thrombin. The system was based on sandwich-type reactions (aptamer-protein-aptamer) to capture the GNPs on the test zone of LFB. The results showed that aptamers performed better than antibodies in accordance with specificity and sensitivity [125]. A competitive aptamer-based LFB was developed to detect β -conglutinin. In the system, the aptamer tended to bind with its complementary DNA sequence than its cognate aptameric target [126]. Aptamer based LFBs have also been employed to detect cancer cells or bacteria cells. Figure 7b shows an aptamer-GNP based LFB for circulating cancer cells. Aptamers selected from live cells by the cell-based SELEX process was conjugated with GNPs. Under the optimal conditions, 4000 Ramos cells can be visually detected within 15 min [127]. In another work, two different aptamers specific for its out-membrane proteins were used to detect *Escherichia coli* O157:H7 (*E. coli* O157:H7). One aptamer was used for magnetic enrichment and the other was utilized as the bacterial cells' signal reporter. After ISDPR amplification of the second aptamer, the generated single-

Table 2 An overview on micro/nano-materials commonly used in as labels in lateral flow biosensors

Kind of Particle	Typical size	Color	Analytes	Ref
Gold nanoparticles	15 ± 3.5 nm	red	thrombin	[125]
Gold nanostars	40 nm	blue	Bisphenol A	[170]
Gold nanocage	50 nm	purple	immunoglobulin G	[171]
Gold-platinum nanoflowers	31 nm	black	immunoglobulin G	[172]
Gold-nanoparticle-decorated silica nanorods	3.4 to 7.0 μm	dark-purple	immunoglobulin G	[118]
silica shell-stabilized gold nanoparticles	17 nm	red	alpha-fetoprotein	[173]
Gold magnetic nanoparticles	32 nm	Red	antigens	[174]
Polystyrene	107 nm	Fluorescent color	antigen	[175]
Liposome	223 nm	Purple	Salmonella	[176]
CdSe/ZnS QDs	25 nm	red fluorescence	Virus	[146]
Upconversion NPs	17 nm, 12 nm	green, blue fluorescence	antigens	[154]
Blue dyes doped latex beads	390 nm	Blue	DNA	[177]
Carbon nanostrings	None	black	influenza	[23]
Carbon nano-strings	100 and 200 nm	gray/black	DNA	[178]
Carbon nanoparticle	average 120 nm	black	thiabendazole	[179]
Fluorescent carbon nanoparticle	15 nm	fluorescence	DNA	[180]
Carbon nanotube	0.5–2 μm	Black	DNA	[181]
Magnetic carbon nanotube	3 to 5 μm	Black	CA 19–9	[68]
Europium (III) Chelate Microparticles	0.12 and 0.21 μm	far red fluorescence	Eosinophils and Neutrophils	[182]
Green nanoparticle	0.42 μm	green	virus	[183]
Magnetic nanoparticle	10.1 ± 1.5 nm	Dark brown	Pesticide	[184]
SERS	40 nm	SERS spectrum	antibiotics	[160]

strand DNAs were detected in a LFB, resulted in that a minimum of *E. coli* O157:H7 of 10 colony forming units (CFU) was detected [128].

The detection of metal ions on the LFB can be turned into DNA detection as well through molecular recognition element (Fig. 7c). Metal ion-dependent DNA-cleaving DNAszymes

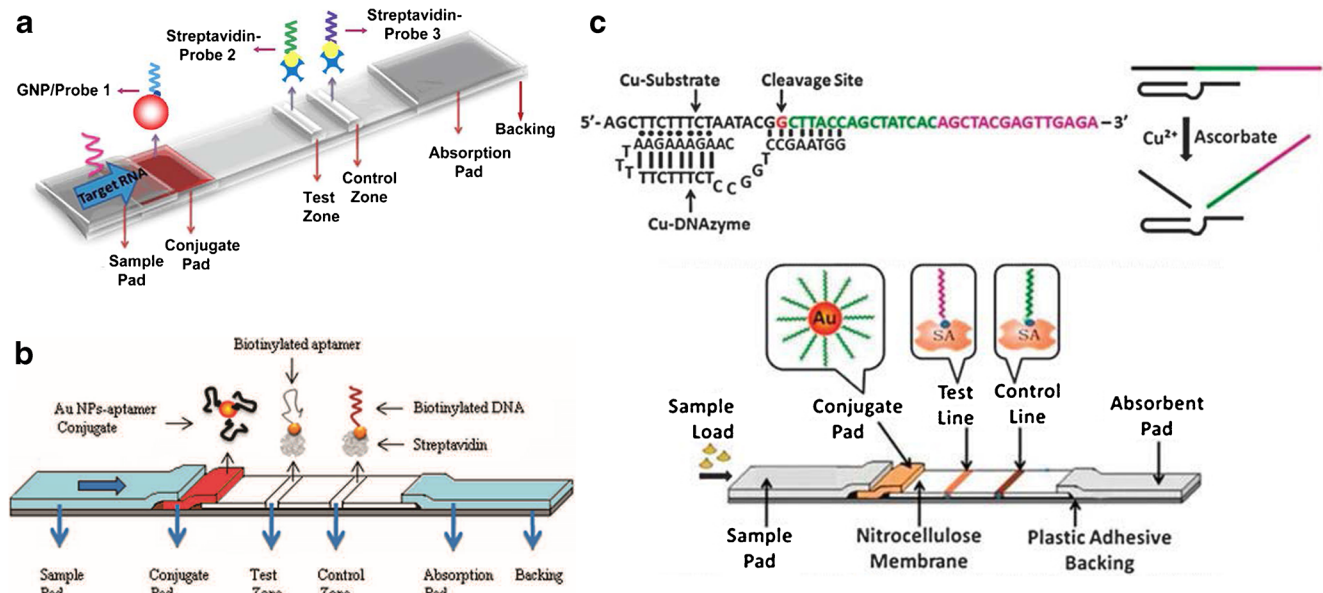


Fig. 7 **a** LFB with DNA probe conjugated with GNPs for microRNA. Reproduced with permission from reference [116]. **b** LFB with aptamer conjugated with GNPs for thrombin detection. Reproduced with

permission from reference [127]. **c** LFB with DNA probe conjugated with GNPs for Cu²⁺. Reproduced with permission from reference [132]

were used to prepare the LFBs for Pb^{2+} and Cu^{2+} . In the presence of Pb^{2+} or Cu^{2+} , one chain of the double-strand DNAzyme catalyzed the cleavage of the other chain at the specific base into two small ssDNA fragments. The ssDNAs were further detected in the GNP-based LFBs. The detection limit of Pb^{2+} and Cu^{2+} was 5 μM and 10 nM, respectively [121, 123]. Following these two works, another LFB was proposed for Pb^{2+} with an enzyme-free DNA amplification circuit based on the Pb^{2+} specific DNA enzyme. After the cleavage, the produced ssDNAs were added to the enzyme-free DNA circuit, through which signal transaction and amplification were conducted. The LOD is 10 pM, with an improvement of four orders of magnitude compared to the above work [122].

Traditional color-based strip reader is based on a digital camera to take the images. A computer (lab top) is required for data processing. Recently, smartphone have been applied for the quantitative determination of LFBs. There are more than 2 billion smartphone users in the world [18]. Since modern smartphones are not only portable and wireless telecommunication infrastructure but are also equipped with digital components such as high-performance camera/imaging module, LCD displays, and various receivers/transmitters, they have provided stimulating opportunities and become the favored tool for use in many POCT applications. Recently, cell phones have been used with LFBs to detect hormones, disease-related markers, stress related biomarkers, pesticides, etc. (Table 3). The combination of mobile phones with 3D printing technology and wireless information technology has indicated great prospects in POCT and greatly improved the diagnosis, treatment and prognosis of diseases.

In one work, smartphone was integrated with GNP-based LFBs to detect infectious diseases with a compact digital RDT reader. The reader weighs only about 65 g and is mechanically connected to the smartphone to align the camera portion of the phone. Various types of LFBs can be inserted into the reader and imaged in reflective or transmissive mode by the phone's own illumination. The raw image of the captured tests can be then digitally processed by the smart app on the smartphone and the diagnostic results can be automatically read. The smart application then sends the resulting data, LFB images, and other relevant information (eg. patient information, time, location, etc.) to the central server, which displays the diagnostic results on the world map by geotagging. This makes it easy to view time and space dynamic maps of a disease using an internet browser or smartphone app [129]. In another work, a smartphone based LFB was described for semi-quantitative determination of thyroid stimulating hormone. It had an attachment printed by a 3D printer to collect LFBs and smartphones with a specially designed APP for image analysis, data handling and storage [130]. The general used smart phone holder was criticized to be relatively heavy and very expensive to

manufacture. To overcome these limitations, an origami smartphone holder was fabricated. The weight, fabrication time and cost were reduced about two folds, 11 folds and 100 folds, respectively. The experiment results showed that the ambient light was efficiently blocked out by origami smartphone holder [131].

Luminescent based LFBs and smartphone/luminescence-based LFBs

Traditional LFBs are based on labeled colloidal gold or latex particles, the analyte is visually detected through color presentation in definite strip zones. However, this approach provides limited value for quantitative diagnosis and the sensitivity is criticized below required standard. LFBs with photoluminescent labels such as chemiluminescence and fluorescent nanoparticles (quantum dots) have showed great improvement in sensitivity and dynamic range [132–142]. Zhang et al. reported a portable fluorescent silica nanoparticle based LFB for Clenbuterol (CL) with a visual detection limit of 0.1 ng mL⁻¹, which indicated the sensitivity of the fluorescent silica nanoparticle -based LFBs was better than that of conventional GNP-based LFBs [132]. Luminescence nanoparticles (PLNPs) was used as the reporter of the LFB with the enhancement in sensitivity, photobleaching resistance, quantitation amenability and bioconjugation schemes design. Such LFBs using the NeutrAvidin PLNPs was approximately ten times more sensitive than using GNPs [135]. In the work related to a chemiluminescent LFB, the LOD of the CL-based results is 20 times lower than that of the bare-eye readout [143]. Moreover, a chemiluminescence-based LFB was described for monitoring astronauts' health, which was successfully used by an Italian astronaut during a space mission [144]. Özalp et al. introduced a horse radish peroxidase (HRP) based LFB for reactive oxygen species (ROS). HRP together with Texas Red dextran were encapsulated inside the porous polyacrylamide nanoparticles. By this way, enzymes were protected in the porous matrix of polyacrylamide but the analyte can freely pass in and out, providing a general strategy for enzyme-based LFB [133].

Likewise, QDs are better labels against organic fluorophores because of their high levels of brightness, size-tunable fluorescence emission, large absorption coefficients, etc. [29, 136, 145]. QDs are often used in the LFBs as one kind of promising fluorescent nanoparticles. QDs earlier presented as a reporter of LFB in Lin et al.'s work. Recently, a carboxyl functionalized QDs-embedded silica nanoparticles labeled LFB was demonstrated for procalcitonin (PCT) antigens. The visual detection limit of fluorescence nanoparticles for PCT antigens counted about two hundred times higher than GNPs-based method [136]. In another QDs based LFB, two influenza A virus subtypes H5 and H9 were simultaneously detected on one

Table 3 Smartphone-based lateral flow biosensors

Tracer	Analyte(s)	Detection method	Mobile Device	Attachment	Other remarks	Ref.
GNPs	Malaria, tuberculosis and HIV RDTs	Colorimetric	Samsung Galaxy S II	Cost-effective digital RDT reader, weighing only ~65 g	Various results can be viewed and shared using internet browsers and smartphone	[129]
GNPs	hormone	Colorimetric	iOS application	Attachment designed by Solidworks, and printed by a 3D printer	Using the methodology of the optimized Rayleigh/Mie scatterer detection	[130]
Luminol/enhancer/hydrogenperoxide	Salivary cortisol	Chemiluminescence	Samsung Galaxy SII Plus	Attachment designed by Tinkercad, and printed by Makerbot	A mini-darkbox and aligned optical interface between the camera and the LFIA membrane	[149]
Latex	Avian influenza	Fluorescence	Samsung, Galaxy S3	Attachment printed by a 3D printer Replicator	The excitation and emission wavelength are 460 or 560 nm, respectively.	[150]
GNPs and fluorescent labels	Gonadotropin and carcinoembryonic antigen	Colorimetric/Fluorescence	Red Mi Note 2 smart phone	Attachment designed by SolidWorks software and fabricated using a 3D printer	Smartphone-controlled dual-modality imaging system.	[185]
GNPs	Cortisol and C-reactive protein	Colorimetric	Galaxy S3 LTE	Smartphone holder made by origami	A paper-based origami smartphone holder to reduce cost and manufacturing time	[131]
Upconversion nanoparticles	brain natriuretic peptide and suppression of tumorigenicity 2	Fluorescence	Three smartphones Redmi Note, Mi 5, and 360 N 4 s	None	Reader composed of a smartphone, top cover, optical system, power supply, and bottom cover	[154]
QDs	Chlorpyrifos, diazinon, and malathion	Fluorescence	iPhone 5	Reader printed by a 3D printer	Reader equipped with an excitation laser source, power, sample cascade, and fluorescence imaging optics	[155]
QDs microspheres	Zika virus nonstructural protein 1	Fluorescence	Nokia Lumia 1020	Attachment designed using SolidWorks software and 3D-printed	Platform consists of a smartphone, a excitation light source, optical filters, an external lens, power unit, and a 3D-printed plastic.	[153]
GNPs	Digoxigenin	Colorimetric	iPhone 5S	A simple darkbox made from black cardboard	None	[186]

LFB without interferences [146]. Fluorescence quenching of CdSe/ZnS QDs in the presence of gold and silver nanoparticles were used to develop QDs-based LFBs. The visual LOD is three orders lower than that of colorimetric detection methods [147]. In another QDs based LFB, UV protective goggles under UV lamp was used to observe the results with a detection limit of 25 ng mL^{-1} , and the quantitative results can be obtained with a gel imager [148].

The chemical response from luminescent nanoparticles can be conveniently converted into electrical signal via mobile phone apps with certain devices [129, 130, 149]. Compared with other methods, the mobile phone-based approach introduces front-end technology (smartphones and networks) into LFB, which improves the convenience of LFB detection; moreover, it has advantages in generating sensitive and quantitative information. As a consequence, it has foreseeable prospect future in home-self-diagnostic device industry. A chemiluminescent (CL) based LFB incorporated in a smart phone for quantitative detection of salivary cortisol was demonstrated in Fig. 8 [149]. Such biosensor is based on a competitive immune assay utilizing peroxidase–cortisol conjugate. The mobile webcam played a role of light detector to acquire image signals, which would be processed through mobile phone apps. The complete system incorporated a cartridge for LFBs to be placed, a 3D-printed smart phone fixing adaptor, a plano-convex lens and a cartridge-insertion slot. This configuration imitated a small dark box and optical interface for phone cameras generating CL signals. The advantage

of this assay was simple to conduct and instant for result. The detecting range was $0.3\text{--}60 \text{ ng mL}^{-1}$, which complies with accepted clinically criteria for salivary cortisol detection.

Likewise, RDT reader and mobile phone were used for sensing analytes in multiple LFBs. Compared to the above work, the information from the mobile phone can be easily shared to a central server by internet to draw a dynamically updating diagnostic information world map. This idea can open a new page for other RDT as well. The real-time updating spatio-temporal information system for diseases can be established by data generated from mobile apps, which would contribute dramatically to global epidemics control [129]. The clinical performance of a smartphone-based fluorescent LFB was assessed. The light collection efficiency was improved using a reflective light collection module. This is very important when fluorescence excitation is battery-operated. Besides, the performance of the smartphone device was even two times better than that of the benchtop fluorescence reader which is much bigger and more expensive [150]. A similar power-free and portable device was described to detect QDs signals. The tumor marker carcinoembryonic antigen (CEA) was detected with a detection range of $1\text{--}100 \text{ ng mL}^{-1}$ and detection limit of 0.049 ng mL^{-1} [151]. Following these works, luminescence-based LFBs have been reported for the detection of various targets, including nucleic acids [152], virus protein [153], cardiovascular diseases biomarkers [154], multi-pesticides [155], and glutathione [156].

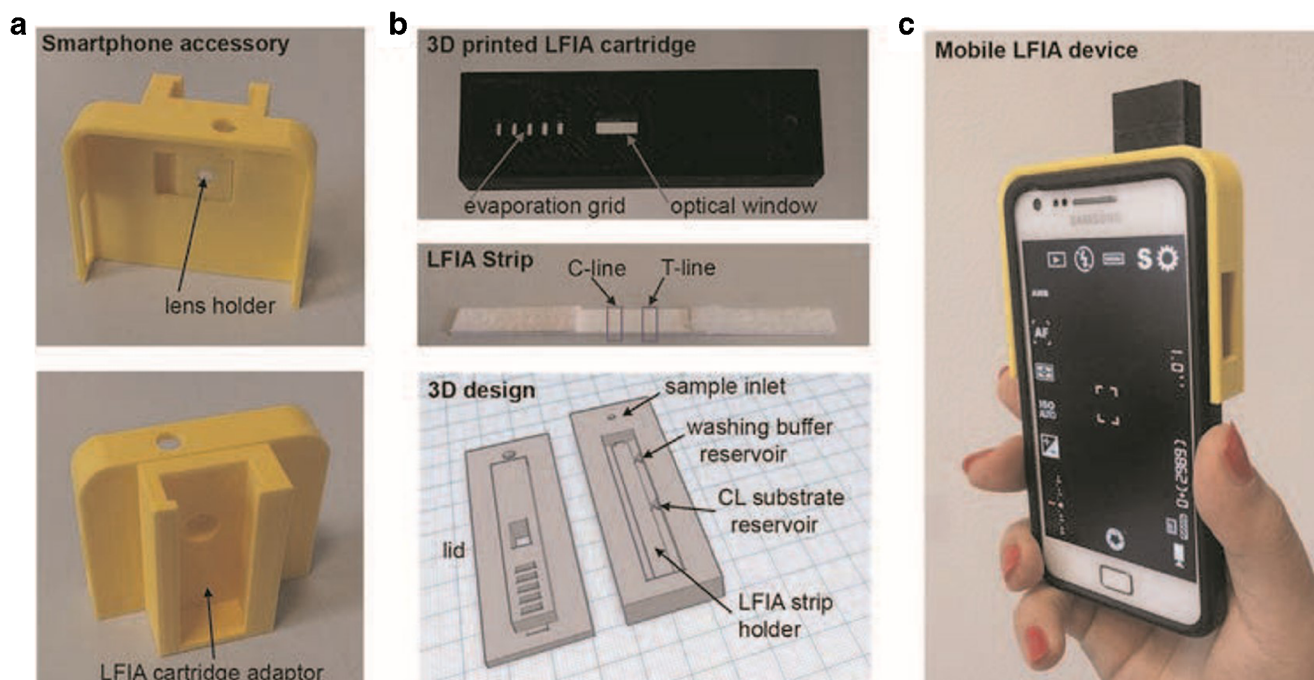


Fig. 8 **a** 3D printed smart phone accessory. **b** 3D printed cartridge. **c** The integrated cortisol LFB smart phone-based device for salivary cortisol. Reproduce with permission reference from reference [149]

SERS based lateral flow biosensors (LFBs)

As promising as the smartphone-luminescent-based LFBs there are still some drawbacks: the fluorescence signals can be easily interfered by substantial from the blood and tissue fluid; it is difficult to achieve high accuracy at low target rates free from false result; the analytic systems is not small and light enough to be convenient enough as a point-of-care and home-use diagnosis method. To overcome the drawbacks mentioned above, surface-enhanced raman spectroscopy (SERS) readers are employed for the quantitative determination of LFBs.

Raman signal intensity gets enhanced when molecules are absorbed on metal nanoparticles, colloids and rough surfaces, so a SERS response is obtained. SERS has some unique advantages, such as spectral fingerprint of targets; no interference from water; single molecule sensitivity; easy sample preparation and operation; multiplexing capability [160]. Besides the SERS-based LFB we mentioned above [43, 161, 162], in the

last few years, different groups have developed SERS-based LFBs based on antigen-antibody interactions and nucleic acid hybridization for hormone, toxin, bacterial, virus, pesticide and so on (Table 4). The limitation of detection sensitivity and quantitative analysis were greatly addressed, with the improvement of the sensitivity for 2 to 4 orders of magnitude compared with the conventional colorimetric LFB. Besides, SERS-based LFBs was demonstrated to have much better selectivity than the colorimetric counterpart when they were applied to the blood plasma sample matrix [100]. Choo's group developed SERS-based LFBs for HIV-1 DNA, staphylococcal enterotoxin B, thyroid-stimulating hormone and dual nucleic acids [157, 162–164]. Such SERS-based LFBs were two order to four orders more sensitive than colorimetric, ELISA or fluorescent methods. The SERS-based LFB was used for the detection of dual nucleic acids targets (Fig. 9a). The detection limit was four orders lower than that obtained with the aggregation-based colorimetric method [157]. A nonspherical gap-enhanced Raman tags with strong and uniform SERS response was used

Table 4 SERS-based lateral flow biosensors

tracer	Analyte(s)	Detection mode	Detection method	Analytical sensitivities	Ref.
Malachite green isothiocyanate-functionalized AuNPs	HIV-1DNA	Nucleic acid hybridization	Colorimetric, SERS	0.24 pg mL ⁻¹	[162]
Malachite green isothiocyanate functionalized hollow gold nanospheres	<i>Staphylococcal enterotoxin B</i>	Antigen-antibody interactions	Colorimetric, SERS	0.001 ng mL ⁻¹	[163]
Flucytosine	Flucytosine	Direct detection	Colorimetric, SERS	10 µg mL ⁻¹	[59]
Malachite green isothiocyanate functionalized hollow gold nanospheres	Thyroid-stimulating hormone	Antigen-antibody interactions	Colorimetric, SERS	0.025 IU mL ⁻¹	[164]
Au nanostar @ Raman Reporter @ silica	Neuron-specific enolase	Antigen-antibody interactions	Colorimetric, SERS	0.86 ng mL ⁻¹	[100]
AuMBA@Ag core-shell nanoparticles	<i>Listeria monocytogenes</i> , <i>Salmonella enterica</i> serotype Enteritidis	Nucleic acid hybridization	Colorimetric, SERS	27 CFU mL ⁻¹ and 19 CFU mL ⁻¹	[187]
SERS Reporter-modified GNPs	Anti-HCV antibodies	Antigen-antibody interactions	Colorimetric, SERS	1/1024 diluted antibody	[43]
SERS Reporter-modified GNPs	Two target DNAs	Nucleic acid hybridization	Colorimetric, SERS	0.043 and 0.074 pM, respectively	[157]
Nonspherical gap-enhanced Raman tags	Troponin I	Antigen-antibody interactions	Colorimetric, SERS	0.1 ng mL ⁻¹	[165]
4-aminothiophenol acid and 4-aminothiophenol labeled AuNPs	Cypermethrin and Esfenvalerate	Antigen-antibody interactions	Colorimetric, SERS	2.3 × 10 ⁻⁴ and 2.6 × 10 ⁻⁵ ng mL ⁻¹ , respectively	[166]
5,5-dithiobis-2-nitrobenzoic acid Labeled gold nanoparticles	Colistin	Antigen-antibody interaction	Colorimetric, SERS	0.10 ng mL ⁻¹	[167]
AuAg ^{4-ATP} @AgNPs	Pseudorabies virus	Antigen-antibody interactions	Colorimetric, SERS	5 ng mL ⁻¹	[168]
Thio-2-naphthol labelled Au/Au core/-satellite nanoparticles	human chorionic gonadotropin	Antigen-antibody interactions	Colorimetric, SERS	1.6 mIU mL ⁻¹	[159]
5,5'-dithiobis(2-nitrobenzoic acid) or 4-Mercaptobutyramidine labelled AuNPs	<i>Listeria monocytogenes</i> and <i>Salmonella typhimurium</i>	Antigen-antibody interactions	Colorimetric, SERS	75 cfu mL ⁻¹ and 75 Cfu mL ⁻¹ , respectively	[169]
AuAg ^{4-ATP} @AgNPs	Avian influenza A	Antigen-antibody interactions	Colorimetric, SERS	0.0018 HAU	[158]

in the LFB. Such SERS tags were an order of magnitude better than that of other common SERS tags in terms of sensitivity, such as Au nanorods, nanostars, nanoshells with surface-adsorbed RMs, or spherical GERTs with embedded RMs [165]. The following works are listed by time. Wang et al. described a SERS-based LFB combined with recombinase polymerase amplification for simultaneous detection of *Listeria monocytogenes* and *Salmonella enterica* serotype Enteritidis [100]. Li et al. developed a SERS-based LFB for the simultaneous detection of two pyrethroid pesticides [166]. Chen developed a SERS-based LFB for colistin in raw milk, the detection limit was far below the ELISA method and the maximum residue limit set by the European Union [167]. Tang et al. described a SERS-based LFB for differential diagnosis of wild-type pseudorabies virus and gE-deleted vaccine. The results from this method were consistent with results from the gE-specific PCR [168]. They also presented a SERS-based LFB for avian influenza A (H7N9) virus, the detection limit of which was three orders lower than that of the corresponding HA assays (Fig. 9b) [158]. Wu et al. developed a SERS-based

LFB for *Listeria monocytogenes* and *Salmonella typhimurium* in milk [169]. All above works demonstrated that SERS-based LFBs has great potential in the point-of-care settings.

In order to improve the major drawback, which is the read-out time until the test result is available for the user, Schlücker et al. designed a portable Raman/SERS-LFB reader using a custom-made fiber optic probe for point-of-care testing of the pregnancy hormone human chorionic gonadotropin, with an LOD of 1.6 mIU mL^{-1} , which is 15-times more sensitive than a commercially available LFB as the gold standard. The acquisition time is only 2–5 s, which is several orders of magnitude shorter than those of existing approaches requiring expensive Raman instrumentation (Fig. 9c). The SERS reader provides stimulating opportunities for cost-effective, quantitative, multiplex and ultrasensitive POCT in real-world application such as clinical chemistry, food and environmental analysis, drug and biowarfare agent testing, etc. [159].

As the recent development we reviewed above, adopting suitable format and new nano-labels, LFBs integrated sample preparation, flow control and detection into one portable device

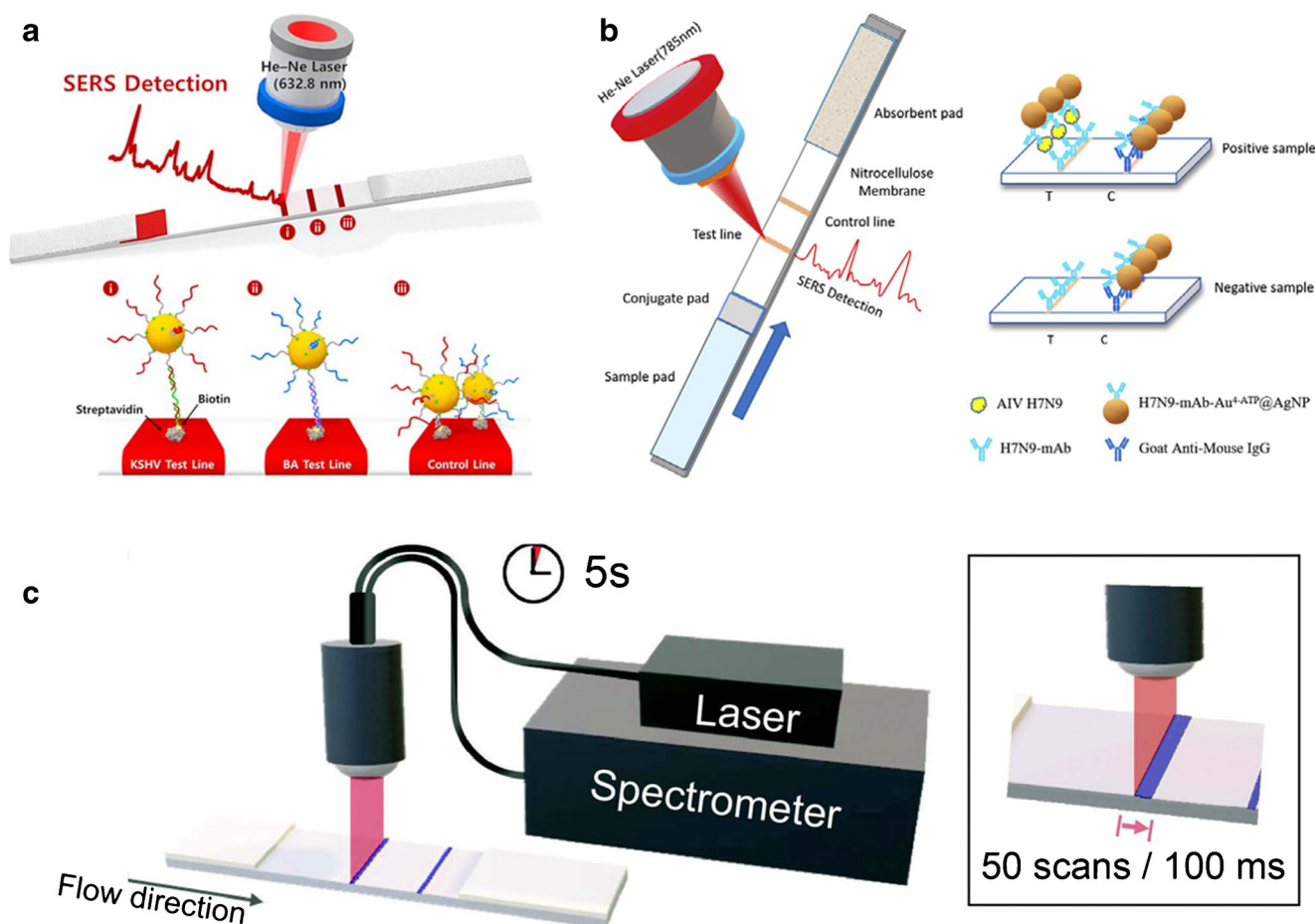


Fig. 9 **a** SERS based LFB for simultaneous detection of dual nucleic acids. Reproduce with permission from reference [157]. **b** SERS based LFB for avian influenza A (H7N9) virus. Reproduce with permission

from reference [158], Elsevier Springer-Verlag Berlin Heidelberg. **c** Schematic representation of a Portable Raman/SERS reader. Reproduce with permission from reference [159]

for sensitive detection in-field and at point-of-care environment may be the tendency of the future LFBs. Under certain circumstance, sample flow in the membranes or some microfluidic arrays, get purified and continue to be detected at the detection region. By this way, the detection is extremely simplified as the result and diagnose information can be obtained by just a drop of samples such as blood or urine in minutes free from interference.

Conclusions and future perspectives

Lateral flow biosensors (LFBs) have proven to be rapid, sensitive, cost-effective methods for point-of-care and in-field diagnosis in resource-limited areas such as developing countries and rural areas. This essay has reviewed the recent development and breakthroughs of the LFBs studies including detection format, sample pretreatment, flow control and reliability. Accordingly, latest research indicate that there is still plenty of room to develop the LFBs with smaller demand volume, shorter analysis time and the absence of hook effect, and higher accuracy and sensitivity.

Even though booming development of the LFBs has been witnessed in the last decade, there are still some implementing issues to be resolved before LFBs are made into mature commercial products. First of all, the sample volume is demanded to be smaller. A drop of liquid such as blood or tissue fluid is strongly suggested. Secondly, for the purpose of commercial use, sensitivity of LFBs is supposed to be high enough to reach the market requirement. Most importantly, the substance in blood or tissue fluid should not interfere the signal. Facing these problems, first of all, appropriate materials for sample pretreatment and signal labels need to be developed. Secondly, detection format like cotton- and VFA-based LFBs need to be improved to make the detection volume smaller and quicker with high reliability. Thirdly, flow control strategy like cross-flow, delayed release, controlled release strategy should be improved in terms of simplification, convenience and multiplex. Lastly foreseeable, to make the detection systems of the LFB portable, energy-free, cost-effective and easy for mass production is a challenge to be resolved. Conclude from above, we still have a long way to go before the next generation of the LFBs goes as we expected.

Acknowledgements This research was supported by the National Institute of Health, Centers of Biomedical Research Excellence (NIH, COBRE, Grant number: P20 GM109024), the National Natural Science Foundation of China (Grant No. 31700735), the National Natural Science Foundation of Anhui Province (Grant No: 1908085 MB54, 1808085QH264), the Beijing Natural Science Foundation (Grant No. 2122038), Wanjiang scholar Award of Anhui Province, Basic research business fund of central universities (FRF-TP-18-020A1), China Postdoctoral Science Foundation (2018 M631332).

Compliance with ethical standards

Conflict of interest The author(s) declare that they have no competing interests.

References

- Glad C, Grubb A (1981) Immunocapillary migration with enzyme labeled antibodies: rapid quantification of C-reactive protein in human plasma. *Anal Biochem* 116(2):6. [https://doi.org/10.1016/0003-2697\(81\)90367-5](https://doi.org/10.1016/0003-2697(81)90367-5)
- Glynnou K, Ioannou PC, Christopoulos TK, Syriopoulou V (2003) Oligonucleotide-functionalized gold nanoparticles as probes in a dry-reagent strip biosensor for DNA analysis by hybridization. *Anal Chem* 75(16):4155–4160. <https://doi.org/10.1021/ac034256+>
- Xu Y, Liu M, Kong N, Liu J (2016) Lab-on-paper micro- and nano-analytical devices: fabrication, modification, detection and emerging applications. *Microchim Acta* 183(5):1521–1542. <https://doi.org/10.1007/s00604-016-1841-4>
- Quesada-González D, Merkoçi A (2015) Nanoparticle-based lateral flow biosensors. *Biosens Bioelectron* 73:47–63. <https://doi.org/10.1016/j.bios.2015.05.050>
- Huang X, Aguilar ZP, Xu H, Lai W, Xiong Y (2016) Membrane-based lateral flow immunochromatographic strip with nanoparticles as reporters for detection: a review. *Biosens Bioelectron* 75: 166–180. <https://doi.org/10.1016/j.bios.2015.08.032>
- Hu J, Wang S, Wang L, Li F, Pingguan-Murphy B, Lu TJ, Xu F (2014) Advances in paper-based point-of-care diagnostics. *Biosens Bioelectron* 54:585–597. <https://doi.org/10.1016/j.bios.2013.10.075>
- Li J, Macdonald J (2016) Multiplexed lateral flow biosensors: technological advances for radically improving point-of-care diagnoses. *Biosens Bioelectron* 83:177–192. <https://doi.org/10.1016/j.bios.2016.04.021>
- Ge X, Asiri AM, Du D, Wen W, Wang S, Lin Y (2014) Nanomaterial-enhanced paper-based biosensors. *TrAC-Trend Anal Chem* 58:31–39. <https://doi.org/10.1016/j.trac.2014.03.008>
- John A, Price CP (2014) Existing and emerging Technologies for Point-of-Care Testing. *Clin Biochem Rev* 35(3):13
- Gao X, Xu L-P, Zhou S-F, Liu G, Zhang X (2014) Recent Advances in Nanoparticles-based Lateral Flow Biosensors. *Am J Biomed Sci* 6: 41–57. <https://doi.org/10.5099/aj140100041>
- Bamrungsap S, Apiwat C, Chantima W, Dharakul T, Wiriyaichaiyom N (2013) Rapid and sensitive lateral flow immunoassay for influenza antigen using fluorescently-doped silica nanoparticles. *Microchim Acta* 181(1–2):223–230. <https://doi.org/10.1007/s00604-013-1106-4>
- Drygin YF, Blintsov AN, Grigorenko VG, Andreeva IP, Osipov AP, Varitzev YA, Uskov AI, Kravchenko DV, Atabekov JG (2012) Highly sensitive field test lateral flow immunodiagnosics of PVX infection. *Appl Microbiol Biot* 93(1):179–189. <https://doi.org/10.1007/s00253-011-3522-x>
- Hou SY, Hsiao YL, Lin MS, Yen CC, Chang CS (2012) MicroRNA detection using lateral flow nucleic acid strips with gold nanoparticles. *Talanta* 99:375–379. <https://doi.org/10.1016/j.talanta.2012.05.067>
- Jin W, Yamada K, Ikami M, Kaji N, Tokeshi M, Atsumi Y, Mizutani M, Murai A, Okamoto A, Namikawa T, Baba Y, Ohta M (2013) Application of IgY to sandwich enzyme-linked immunosorbent assays, lateral flow devices, and immunopillar chips for detecting staphylococcal enterotoxins in milk and dairy products.

- J Microbiol Meth 92(3):323–331. <https://doi.org/10.1016/j.mimet.2013.01.001>
15. Parolo C, de la Escosura-Muniz A, Merkoci A (2013) Enhanced lateral flow immunoassay using gold nanoparticles loaded with enzymes. *Biosens Bioelectron* 40(1):412–416. <https://doi.org/10.1016/j.bios.2012.06.049>
 16. Pohlmann C, Dieser I, Sprinzl M (2014) A lateral flow assay for identification of *Escherichia coli* by ribosomal RNA hybridisation. *Analyst* 139(5):1063–1071. <https://doi.org/10.1039/c3an02059b>
 17. Xiang T, Jiang Z, Zheng J, Lo C, Tsou H, Ren G, Zhang J, Huang A, Lai G (2012) A novel double antibody sandwich-lateral flow immunoassay for the rapid and simple detection of hepatitis C virus. *Int J Mol Med* 30(5):1041–1047. <https://doi.org/10.3892/ijmm.2012.1121>
 18. Zhu J, Zou N, Zhu D, Wang J, Jin Q, Zhao J, Mao H (2011) Simultaneous detection of high-sensitivity cardiac troponin I and myoglobin by modified sandwich lateral flow immunoassay: proof of principle. *Clin Chem* 57(12):1732–1738. <https://doi.org/10.1373/clinchem.2011.171694>
 19. Fu X, Chu Y, Zhao K, Li J, Deng A (2017) Ultrasensitive detection of the β -adrenergic agonist brombuterol by a SERS-based lateral flow immunochromatographic assay using flower-like gold-silver core-shell nanoparticles. *Microchim Acta* 184(6):1711–1719. <https://doi.org/10.1007/s00604-017-2178-3>
 20. Liu J, Wang J, Li Z, Meng H, Zhang L, Wang H, Li J, Qu L (2018) A lateral flow assay for the determination of human tetanus antibody in whole blood by using gold nanoparticle labeled tetanus antigen. *Microchim Acta* 185(2):110. <https://doi.org/10.1007/s00604-017-2657-6>
 21. Wang W, Liu L, Song S, Xu L, Kuang H, Zhu J, Xu C (2016) Identification and quantification of eight listeria monocytogene serotypes from listeria spp. using a gold nanoparticle-based lateral flow assay. *Microchim Acta* 184(3):715–724. <https://doi.org/10.1007/s00604-016-2028-8>
 22. Tao Y, Yang J, Chen L, Huang Y, Qiu B, Guo L, Lin Z (2018) Dialysis assisted ligand exchange on gold nanorods: amplification of the performance of a lateral flow immunoassay for *E. coli* O157:H7. *Microchim Acta* 185(7):350. <https://doi.org/10.1007/s00604-018-2897-0>
 23. Wiriyaichaiyorn N, Sirikett H, Maneeprakorn W, Dharakul T (2017) Carbon nanotag based visual detection of influenza a virus by a lateral flow immunoassay. *Microchim Acta* 184(6):1827–1835. <https://doi.org/10.1007/s00604-017-2191-6>
 24. Urusov AE, Gubaidullina MK, Petrakova AV, Zherdev AV, Dzantiev BB (2017) A new kind of highly sensitive competitive lateral flow immunoassay displaying direct analyte-signal dependence. Application to the determination of the mycotoxin deoxynivalenol. *Microchim Acta* 185(1):29. <https://doi.org/10.1007/s00604-017-2576-6>
 25. Li SJ, Sheng W, Wen W, Gu Y, Wang JP, Wang S (2018) Three kinds of lateral flow immunochromatographic assays based on the use of nanoparticle labels for fluorometric determination of zearalenone. *Microchim Acta* 185(4):238. <https://doi.org/10.1007/s00604-018-2778-6>
 26. Wang Y, Wang L, Zhang C, Liu F (2019) A lateral flow assay for copper(II) utilizing catalytic and stem-loop based signal amplification. *Microchim Acta* 186(2):82. <https://doi.org/10.1007/s00604-018-3197-4>
 27. Zhong Y, Chen Y, Yao L, Zhao D, Zheng L, Liu G, Ye Y, Chen W (2016) Gold nanoparticles based lateral flow immunoassay with largely amplified sensitivity for rapid melamine screening. *Microchim Acta* 183(6):1989–1994. <https://doi.org/10.1007/s00604-016-1812-9>
 28. Mao X, Ma Y, Zhang A, Zhang L, Zeng L, Liu G (2009) Disposable nucleic acid biosensors based on gold nanoparticle probes and lateral flow strip. *Anal Chem* 81(4):1660–1668. <https://doi.org/10.1021/ac8024653>
 29. Li Z, Wang Y, Wang J, Tang Z, Pounds JG, Lin Y (2010) Rapid and sensitive detection of protein biomarker using a portable fluorescence biosensor based on quantum dots and a lateral flow test strip. *Anal Chem* 82(16):7008–7014. <https://doi.org/10.1021/ac101405a>
 30. Wang DB, Tian B, Zhang ZP, Deng JY, Cui ZQ, Yang RF, Wang XY, Wei HP, Zhang XE (2013) Rapid detection of bacillus anthracis spores using a super-paramagnetic lateral-flow immunological detection system. *Biosens Bioelectron* 42:661–667. <https://doi.org/10.1016/j.bios.2012.10.088>
 31. Li X, Tian J, Shen W (2010) Thread as a versatile material for low-cost microfluidic diagnostics. *ACS Appl Mater Inter* 2(1):1–6. <https://doi.org/10.1021/am9006148>
 32. Reches M, Mirica KA, Dasgupta R, Dickey MD, Butte MJ, Whitesides GM (2010) Thread as a matrix for biomedical assays. *ACS Appl Mater Inter* 2(6):1722–1728. <https://doi.org/10.1021/am1002266>
 33. Safavieh R, Zhou GZ, Juncker D (2011) Microfluidics made of yarns and knots: from fundamental properties to simple networks and operations. *Lab Chip* 11(15):2618–2624. <https://doi.org/10.1039/c1lc20336c>
 34. Zhou G, Mao X, Juncker D (2012) Immunochromatographic assay on thread. *Anal Chem* 84(18):7736–7743. <https://doi.org/10.1021/ac301082d>
 35. Mao X, Du TE, Wang Y, Meng L (2015) Disposable dry-reagent cotton thread-based point-of-care diagnosis devices for protein and nucleic acid test. *Biosens Bioelectron* 65:390–396. <https://doi.org/10.1016/j.bios.2014.10.053>
 36. Mao X, Du TE, Meng L, Song T (2015) Novel gold nanoparticle trimer reporter probe combined with dry-reagent cotton thread immunoassay device for rapid human ferritin test. *Anal Chim Acta* 889:172–178. <https://doi.org/10.1016/j.aca.2015.06.031>
 37. Meng LL, Song TT, Mao X (2017) Novel immunochromatographic assay on cotton thread based on carbon nanotubes reporter probe. *Talanta* 167:379–384. <https://doi.org/10.1016/j.talanta.2017.02.023>
 38. Jia X, Song T, Liu Y, Meng L, Mao X (2017) An immunochromatographic assay for carcinoembryonic antigen on cotton thread using a composite of carbon nanotubes and gold nanoparticles as reporters. *Anal Chim Acta* 969:57–62. <https://doi.org/10.1016/j.aca.2017.02.040>
 39. Wu T, Xu T, Xu LP, Huang Y, Shi W, Wen Y, Zhang X (2016) Superhydrophilic cotton thread with temperature-dependent pattern for sensitive nucleic acid detection. *Biosens Bioelectron* 86:951–957. <https://doi.org/10.1016/j.bios.2016.07.041>
 40. Chen P, Gates-Hollingsworth M, Pandit S, Park A, Montgomery D, AuCoin D, Gu J, Zenhausern F (2019) Paper-based vertical flow immunoassay (VFI) for detection of bio-threat pathogens. *Talanta* 191:81–88. <https://doi.org/10.1016/j.talanta.2018.08.043>
 41. Oh YK, Joung HA, Kim S, Kim MG (2013) Vertical flow immunoassay (VFA) biosensor for a rapid one-step immunoassay. *Lab Chip* 13(5):768–772. <https://doi.org/10.1039/c2lc41016h>
 42. Eltzov E, Marks RS (2017) Colorimetric stack pad immunoassay for bacterial identification. *Biosens Bioelectron* 87:572–578. <https://doi.org/10.1016/j.bios.2016.08.044>
 43. Clarke OJ, Goodall BL, Hui HP, Vats N, Brosseau CL (2017) Development of a SERS-Based rapid vertical flow assay for point-of-care diagnostics. *Anal Chem* 89(3):1405–1410. <https://doi.org/10.1021/acs.analchem.6b04710>
 44. Nunes Pauli GE, de la Escosura-Muniz A, Parolo C, Helmuth Bechtold I, Merkoci A (2015) Lab-in-a-syringe using gold nanoparticles for rapid immunosensing of protein biomarkers. *Lab Chip* 15(2):399–405. <https://doi.org/10.1039/c4lc01123f>
 45. Zor E, Bekar N (2017) Lab-in-a-syringe using gold nanoparticles for rapid colorimetric chiral discrimination of enantiomers.

- Biosens Bioelectron 91:211–216. <https://doi.org/10.1016/j.bios.2016.12.031>
46. Moumita M, Shankar KM, Abhiman PB, Shamasundar BA (2019) Development of a sandwich vertical flow immunogold assay for rapid detection of oxytetracycline residue in fish tissues. *Food Chem* 270:585–592. <https://doi.org/10.1016/j.foodchem.2018.07.124>
47. Bhardwaj J, Shama A, Jang J (2019) Vertical flow-based paper immunosensor for rapid electrochemical and colorimetric detection of influenza virus using a different pore size sample pad. *Biosens Bioelectron* 126:36–43. <https://doi.org/10.1016/j.bios.2018.10.008>
48. Roda A, Zangheri M, Calabria D, Mirasoli M, Caliceti C, Quintavalla A, Lombardo M, Trombini C, Simoni P (2019) A simple smartphone-based thermochemiluminescent immunosensor for valproic acid detection using 1,2-dioxetane analogue-doped nanoparticles as a label. *Sensor Actuat B-Chem* 279:327–333. <https://doi.org/10.1016/j.snb.2018.10.012>
49. Nybond S, Reu P, Rhedin S, Svedberg G, Alfven T, Gantelius J, Svahn HA (2019) Adenoviral detection by recombinase polymerase amplification and vertical flow paper microarray. *Anal Bioanal Chem* 411(4):813–822. <https://doi.org/10.1007/s00216-018-1503-y>
50. Joung HA, Ballard ZS, Ma A, Tseng DK, Teshome H, Burakowski S, Garner OB, Di Carlo D, Ozcan A (2019) Paper-based multiplexed vertical flow assay for point-of-care testing. *Lab Chip* 19(6):1027–1034. <https://doi.org/10.1039/c9lc00011a>
51. Wang KY, Bu SJ, Ju CJ, Han Y, Ma CY, Liu WS, Li ZY, Li CT, Wan JY (2019) Disposable syringe-based visual immunotest for pathogenic bacteria based on the catalase mimicking activity of platinum nanoparticle-concanavalin a hybrid nanoflowers. *Microchim Acta* 186(2):57. <https://doi.org/10.1007/s00604-018-3133-7>
52. Henriksen K, O'Bryant SE, Hampel H, Trojanowski JQ, Montine TJ, Jeromin A, Blennow K, Lonnberg A, Wyss-Coray T, Soares H, Bazenet C, Sjogren M, Hu W, Lovestone S, Karsdal MA, Weiner MW, Blood-Based Biomarker Interest G (2014) The future of blood-based biomarkers for Alzheimer's disease. *Alzheimers Dement* 10(1):115–131. <https://doi.org/10.1016/j.jalz.2013.01.013>
53. Cheng YS, Rees T, Wright J (2014) A review of research on salivary biomarkers for oral cancer detection. *Clin Trans Med* 3(1):3. <https://doi.org/10.1186/2001-1326-3-3>
54. Gonzalez JM, Foley MW, Bieber NM, Bourdelle PA, Niedbala RS (2011) Development of an ultrasensitive immunochromatography test to detect nicotine metabolites in oral fluids. *Anal Bioanal Chem* 400(10):3655–3664. <https://doi.org/10.1007/s00216-011-5051-y>
55. Lopez Marzo AM, Pons J, Blake DA, Merkoci A (2013) All-integrated and highly sensitive paper based device with sample treatment platform for Cd²⁺ immunodetection in drinking/tap waters. *Anal Chem* 85(7):3532–3538. <https://doi.org/10.1021/ac3034536>
56. Worsley GJ, Attree SL, Noble JE, Horgan AM (2012) Rapid duplex immunoassay for wound biomarkers at the point-of-care. *Biosens Bioelectron* 34(1):215–220. <https://doi.org/10.1016/j.bios.2012.02.005>
57. Rohman B, Richards-Kortum R (2015) Inhibition of recombinase polymerase amplification by background DNA: a lateral flow-based method for enriching target DNA. *Anal Chem* 87(3):1963–1967. <https://doi.org/10.1021/ac504365v>
58. Tang R, Yang H, Choi JR, Gong Y, Hu J, Feng S, Pingguan-Murphy B, Mei Q, Xu F (2016) Improved sensitivity of lateral flow assay using paper-based sample concentration technique. *Talanta* 152:269–276. <https://doi.org/10.1016/j.talanta.2016.02.017>
59. Berger AG, Restaino SM, White IM (2017) Vertical-flow paper SERS system for therapeutic drug monitoring of flucytosine in serum. *Anal Chim Acta* 949:59–66. <https://doi.org/10.1016/j.aca.2016.10.035>
60. Moghadam BY, Connelly KT, Posner JD (2014) Isotachophoretic preconcentration on paper-based microfluidic devices. *Anal Chem* 86(12):5829–5837. <https://doi.org/10.1021/ac500780w>
61. Moghadam BY, Connelly KT, Posner JD (2015) Two orders of magnitude improvement in detection limit of lateral flow assays using isotachopheresis. *Anal Chem* 87(2):1009–1017. <https://doi.org/10.1021/ac504552r>
62. Chen F, Ming X, Chen X, Gan M, Wang B, Xu F, Wei H (2014) Immunochromatographic strip for rapid detection of Cronobacter in powdered infant formula in combination with silica-coated magnetic nanoparticles separation and 16S rRNA probe. *Biosens Bioelectron* 61:306–313. <https://doi.org/10.1016/j.bios.2014.05.033>
63. Fang Z, Wu W, Lu X, Zeng L (2014) Lateral flow biosensor for DNA extraction-free detection of Salmonella based on aptamer mediated strand displacement amplification. *Biosens Bioelectron* 56:192–197. <https://doi.org/10.1016/j.bios.2014.01.015>
64. Wang DB, Tian B, Zhang ZP, Wang XY, Fleming J, Bi LJ, Yang RF, Zhang XE (2015) Detection of bacillus anthracis spores by super-paramagnetic lateral-flow immunoassays based on "road closure". *Biosens Bioelectron* 67:608–614. <https://doi.org/10.1016/j.bios.2014.09.067>
65. Lu X, Liang X, Dong J, Fang Z, Zeng L (2016) Lateral flow biosensor for multiplex detection of nitrofurantol metabolites based on functionalized magnetic beads. *Anal Bioanal Chem* 408(24):6703–6709. <https://doi.org/10.1007/s00216-016-9787-2>
66. Davis KM, Gibson LE, Haselton FR, Wright DW (2014) Simple sample processing enhances malaria rapid diagnostic test performance. *Analyst* 139(12):3026–3031. <https://doi.org/10.1039/c4an00338a>
67. Huang Y, Wen Y, Baryeh K, Takalkar S, Lund M, Zhang X, Liu G (2017) Magnetized carbon nanotubes for visual detection of proteins directly in whole blood. *Anal Chim Acta* 993:79–86. <https://doi.org/10.1016/j.aca.2017.09.025>
68. Huang Y, Wen Y, Baryeh K, Takalkar S, Lund M, Zhang X, Liu G (2017) Lateral flow assay for carbohydrate antigen 19-9 in whole blood by using magnetized carbon nanotubes. *Microchim Acta* 184(11):4287–4294. <https://doi.org/10.1007/s00604-017-2464-0>
69. Sharma A, Tok AIY, Lee C, Ganapathy R, Alagappan P, Liedberg B (2019) Magnetic field assisted preconcentration of biomolecules for lateral flow assaying. *Sensor Actuat B Chem* 285:431–437. <https://doi.org/10.1016/j.snb.2019.01.073>
70. Ren W, Mohammed SI, Wereley S, Irudayaraj J (2019) Magnetic focus lateral flow sensor for detection of cervical Cancer biomarkers. *Anal Chem* 91(4):2876–2884. <https://doi.org/10.1021/acs.analchem.8b04848>
71. Kim TH, Park J, Kim CJ, Cho YK (2014) Fully integrated lab-on-a-disc for nucleic acid analysis of food-borne pathogens. *Anal Chem* 86(8):3841–3848. <https://doi.org/10.1021/ac403971h>
72. Park BH, Oh SJ, Jung JH, Choi G, Seo JH, Kim DH, Lee EY, Seo TS (2017) An integrated rotary microfluidic system with DNA extraction, loop-mediated isothermal amplification, and lateral flow strip based detection for point-of-care pathogen diagnostics. *Biosens Bioelectron* 91:334–340. <https://doi.org/10.1016/j.bios.2016.11.063>
73. Choi JR, Hu J, Tang R, Gong Y, Feng S, Ren H, Wen T, Li X, Wan Abas WA, Pingguan-Murphy B, Xu F (2016) An integrated paper-based sample-to-answer biosensor for nucleic acid testing at the point of care. *Lab Chip* 16(3):611–621. <https://doi.org/10.1039/c5lc01388g>
74. Nilghaz A, Guan L, Tan W, Shen W (2016) Advances of paper-Based microfluidics for diagnostics—the original motivation and

- current status. *ACS Sensors* 1(12):1382–1393. <https://doi.org/10.1021/acssensors.6b00578>
75. Cho JH, Han SM, Paek EH, Cho IH, Paek SH (2006) Plastic ELISA-on-a-chip based on sequential cross-flow chromatography. *Anal Chem* 78(3):793–800. <https://doi.org/10.1021/ac051453v>
76. Cho IH, Seo SM, Paek EH, Paek SH (2010) Immunogold-silver staining-on-a-chip biosensor based on cross-flow chromatography. *J Chromatogr B* 878(2):271–277. <https://doi.org/10.1016/j.jchromb.2009.07.016>
77. Park JN, Paek SH, Kim DH, Seo SM, Lim GS, Kang JH, Paek SP, Cho IH, Paek SH (2016) Conformation-sensitive antibody-based point-of-care immunosensor for serum ca(2+) using two-dimensional sequential binding reactions. *Biosens Bioelectron* 85:611–617. <https://doi.org/10.1016/j.bios.2016.05.061>
78. Fu E, Liang T, Houghtaling J, Ramachandran S, Ramsey SA, Lutz B, Yager P (2011) Enhanced sensitivity of lateral flow tests using a two-dimensional paper network format. *Anal Chem* 83(20):7941–7946. <https://doi.org/10.1021/ac201950g>
79. Shin JH, Park JK (2016) Functional packaging of lateral flow strip allows simple delivery of multiple reagents for multistep assays. *Anal Chem* 88(21):10374–10378. <https://doi.org/10.1021/acs.analchem.6b02869>
80. Joung HA, Oh YK, Kim MG (2014) An automatic enzyme immunoassay based on a chemiluminescent lateral flow immunosensor. *Biosens Bioelectron* 53:330–335. <https://doi.org/10.1016/j.bios.2013.10.004>
81. Akanda MR, Joung HA, Tamilavan V, Park S, Kim S, Hyun MH, Kim MG, Yang H (2014) An interference-free and rapid electrochemical lateral-flow immunoassay for one-step ultrasensitive detection with serum. *Analyst* 139(6):1420–1425. <https://doi.org/10.1039/c3an02328a>
82. Kim K, Joung HA, Han GR, Kim MG (2016) An immunochromatographic biosensor combined with a water-swallowable polymer for automatic signal generation or amplification. *Biosens Bioelectron* 85:422–428. <https://doi.org/10.1016/j.bios.2016.04.096>
83. Kim W, Lee S, Jeon S (2018) Enhanced sensitivity of lateral flow immunoassays by using water-soluble nanofibers and silver-enhancement reactions. *Sensor Actuat B Chem* 273:1323–1327. <https://doi.org/10.1016/j.snb.2018.07.045>
84. Preechakasedkit P, Siangproh W, Khongchareonporn N, Ngamrojanavanich N, Chailapakul O (2018) Development of an automated wax-printed paper-based lateral flow device for alpha-fetoprotein enzyme-linked immunosorbent assay. *Biosens Bioelectron* 102:27–32. <https://doi.org/10.1016/j.bios.2017.10.051>
85. Fu E, Kauffman P, Lutz B, Yager P (2010) Chemical signal amplification in two-dimensional paper networks. *Sensors Actuators B Chem* 149(1):325–328. <https://doi.org/10.1016/j.snb.2010.06.024>
86. Fu E, Liang T, Spicar-Mihalic P, Houghtaling J, Ramachandran S, Yager P (2012) Two-dimensional paper network format that enables simple multistep assays for use in low-resource settings in the context of malaria antigen detection. *Anal Chem* 84(10):4574–4579. <https://doi.org/10.1021/ac300689s>
87. Fridley GE, Le HQ, Fu E, Yager P (2012) Controlled release of dry reagents in porous media for tunable temporal and spatial distribution upon rehydration. *Lab Chip* 12(21):4321–4327. <https://doi.org/10.1039/c2lc40785j>
88. Fridley GE, Le H, Yager P (2014) Highly sensitive immunoassay based on controlled rehydration of patterned reagents in a 2-dimensional paper network. *Anal Chem* 86(13):6447–6453. <https://doi.org/10.1021/ac500872j>
89. Koo CK, He F, Nugen SR (2013) An inkjet-printed electrowetting valve for paper-fluidic sensors. *Analyst* 138(17):4998–5004. <https://doi.org/10.1039/c3an01114c>
90. Connelly JT, Rolland JP, Whitesides GM (2015) "paper machine" for molecular diagnostics. *Anal Chem* 87(15):7595–7601. <https://doi.org/10.1021/acs.analchem.5b00411>
91. Shen M, Chen Y, Zhu Y, Zhao M, Xu Y (2019) Enhancing the sensitivity of lateral flow immunoassay by centrifugation-assisted flow control. *Anal Chem* 91(7):4814–4820. <https://doi.org/10.1021/acs.analchem.9b00421>
92. Choi JR, Liu Z, Hu J, Tang R, Gong Y, Feng S, Ren H, Wen T, Yang H, Qu Z, Pingguan-Murphy B, Xu F (2016) Polydimethylsiloxane-paper hybrid lateral flow assay for highly sensitive point-of-care nucleic acid testing. *Anal Chem* 88(12):6254–6264. <https://doi.org/10.1021/acs.analchem.6b00195>
93. Yew C-HT, Azari P, Choi JR, Li F, Pingguan-Murphy B (2018) Electrospin-coating of nitrocellulose membrane enhances sensitivity in nucleic acid-based lateral flow assay. *Anal Chim Acta* 1009:81–88. <https://doi.org/10.1016/j.aca.2018.01.016>
94. Oh YK, Joung HA, Han HS, Suk HJ, Kim MG (2014) A three-line lateral flow assay strip for the measurement of C-reactive protein covering a broad physiological concentration range in human sera. *Biosens Bioelectron* 61:285–289. <https://doi.org/10.1016/j.bios.2014.04.032>
95. Zhu X, Shah P, Stoff S, Liu H, Li CZ (2014) A paper electrode integrated lateral flow immunosensor for quantitative analysis of oxidative stress induced DNA damage. *Analyst* 139(11):2850–2857. <https://doi.org/10.1039/c4an00313f>
96. Huang Y, Wang W, Wu T, Xu LP, Wen Y, Zhang X (2016) A three-line lateral flow biosensor for logic detection of microRNA based on Y-shaped junction DNA and target recycling amplification. *Anal Bioanal Chem* 408(28):8195–8202. <https://doi.org/10.1007/s00216-016-9925-x>
97. Ang GY, Yu CY, Yean CY (2012) Ambient temperature detection of PCR amplicons with a novel sequence-specific nucleic acid lateral flow biosensor. *Biosens Bioelectron* 38(1):151–156. <https://doi.org/10.1016/j.bios.2012.05.019>
98. Huang H, Jin L, Yang X, Song Q, Zou B, Jiang S, Sun L, Zhou G (2013) An internal amplification control for quantitative nucleic acid analysis using nanoparticle-based dipstick biosensors. *Biosens Bioelectron* 42:261–266. <https://doi.org/10.1016/j.bios.2012.10.078>
99. Fu Q, Liang J, Lan C, Zhou K, Shi C, Tang Y (2014) Development of a novel dual-functional lateral-flow sensor for on-site detection of small molecule analytes. *Sensor Actuat B Chem* 203:683–689. <https://doi.org/10.1016/j.snb.2014.06.043>
100. Gao X, Zheng P, Kasani S, Wu S, Yang F, Lewis S, Nayeem S, Engler-Chiurazzi EB, Wigginton JG, Simpkins JW, Wu N (2017) Paper-Based surface-enhanced Raman scattering lateral flow strip for detection of neuron-specific enolase in Blood plasma. *Anal Chem* 89(18):10104–10110. <https://doi.org/10.1021/acs.analchem.7b03015>
101. Choi JR, Hu J, Feng S, Wan Abas WA, Pingguan-Murphy B, Xu F (2016) Sensitive biomolecule detection in lateral flow assay with a portable temperature-humidity control device. *Biosens Bioelectron* 79:98–107. <https://doi.org/10.1016/j.bios.2015.12.005>
102. Peng T, Yang W-c, Lai W-H, Xiong Y-H, Wei H, Zhang J (2014) Improvement of the stability of immunochromatographic assay for the quantitative detection of clenbuterol in swine urine. *Anal Methods* 6(18):7394–7398. <https://doi.org/10.1039/c4ay01173b>
103. Sotnikov DV, Zherdev AV, Dzantiev BB (2017) Mathematical model of Serodiagnostic Immunochromatographic assay. *Anal Chem* 89(8):4419–4427. <https://doi.org/10.1021/acs.analchem.6b03635>
104. Schaumburg F, Kler PA, Berli CLA (2018) Numerical prototyping of lateral flow biosensors. *Sensors Actuators B Chem* 259:1099–1107. <https://doi.org/10.1016/j.snb.2017.12.044>

105. Zadehkafi A, Siavashi M, Asiaei S, Bidgoli MR (2019) Simple geometrical modifications for substantial color intensity and detection limit enhancements in lateral-flow immunochromatographic assays. *J Chromatogr B* 1110-1111:1–8. <https://doi.org/10.1016/j.jchromb.2019.01.019>
106. Liu J, Lu Y (2003) A colorimetric lead biosensor using DNAzyme-directed assembly of gold nanoparticles. *J Am Chem Soc* 125(22):6642–6643. <https://doi.org/10.1021/ja034775u>
107. Jia J, Wang B, Wu A, Cheng G, Li Z, Dong S (2002) A method to construct a third-generation horseradish peroxidase biosensor: self-assembling gold nanoparticles to three-dimensional sol-gel network. *Anal Chem* 74(9):2217–2223. <https://doi.org/10.1021/ac011116w>
108. Liu G, Lin YY, Wang J, Wu H, Wai CM, Lin Y (2007) Disposable electrochemical immunosensor diagnosis device based on nanoparticle probe and immunochromatographic strip. *Anal Chem* 79(20):7644–7653. <https://doi.org/10.1021/ac070691i>
109. Guodong L, Mao X, Phillips JA, Xu H, Tan W, Lingwen Z (2009) Aptamer-nanoparticle strip biosensor for sensitive detection of Cancer cells. *Anal Chem* 81:6. <https://doi.org/10.1021/ac901889s>
110. Panferov VG, Safenkova IV, Varitsev YA, Zherdev AV, Dzantiev BB (2017) Enhancement of lateral flow immunoassay by alkaline phosphatase: a simple and highly sensitive test for potato virus X. *Microchim Acta* 185(1):25. <https://doi.org/10.1007/s00604-017-2595-3>
111. He Y, Zeng K, Gurung AS, Baloda M, Xu H, Zhang X, Liu G (2010) Visual detection of single-nucleotide polymorphism with hairpin oligonucleotide-functionalized gold nanoparticles. *Anal Chem* 82(17):7169–7177. <https://doi.org/10.1021/ac101275s>
112. He Y, Zhang S, Zhang X, Baloda M, Gurung AS, Xu H, Zhang X, Liu G (2011) Ultrasensitive nucleic acid biosensor based on enzyme-gold nanoparticle dual label and lateral flow strip biosensor. *Biosens Bioelectron* 26(5):2018–2024. <https://doi.org/10.1016/j.bios.2010.08.079>
113. He Y, Zeng K, Zhang S, Gurung AS, Baloda M, Zhang X, Liu G (2012) Visual detection of gene mutations based on isothermal strand-displacement polymerase reaction and lateral flow strip. *Biosens Bioelectron* 31(1):310–315. <https://doi.org/10.1016/j.bios.2011.10.037>
114. He Y, Zhang X, Zhang S, Kris MK, Man FC, Kawde AN, Liu G (2012) Visual detection of single-base mismatches in DNA using hairpin oligonucleotide with double-target DNA binding sequences and gold nanoparticles. *Biosens Bioelectron* 34(1):37–43. <https://doi.org/10.1016/j.bios.2011.12.055>
115. Lie P, Liu J, Fang Z, Dun B, Zeng L (2012) A lateral flow biosensor for detection of nucleic acids with high sensitivity and selectivity. *Chem Commun* 48(2):236–238. <https://doi.org/10.1039/c1cc15878c>
116. Gao X, Xu H, Baloda M, Gurung AS, Xu LP, Wang T, Zhang X, Liu G (2014) Visual detection of microRNA with lateral flow nucleic acid biosensor. *Biosens Bioelectron* 54:578–584. <https://doi.org/10.1016/j.bios.2013.10.055>
117. Gao X, Xu LP, Wu T, Wen Y, Ma X, Zhang X (2016) An enzyme-amplified lateral flow strip biosensor for visual detection of microRNA-224. *Talanta* 146:648–654. <https://doi.org/10.1016/j.talanta.2015.06.060>
118. Xu H, Chen J, Birrenkott J, Zhao JX, Takalkar S, Baryeh K, Liu G (2014) Gold-nanoparticle-decorated silica nanorods for sensitive visual detection of proteins. *Anal Chem* 86(15):7351–7359. <https://doi.org/10.1021/ac502249f>
119. Fang Z, Ge C, Zhang W, Lie P, Zeng L (2011) A lateral flow biosensor for rapid detection of DNA-binding protein c-Jun. *Biosens Bioelectron* 27(1):192–196. <https://doi.org/10.1016/j.bios.2011.06.014>
120. He Y, Zhang X, Zeng K, Zhang S, Baloda M, Gurung AS, Liu G (2011) Visual detection of hg(2)(+) in aqueous solution using gold nanoparticles and thymine-rich hairpin DNA probes. *Biosens Bioelectron* 26(11):4464–4470. <https://doi.org/10.1016/j.bios.2011.05.003>
121. Fang Z, Huang J, Lie P, Xiao Z, Ouyang C, Wu Q, Wu Y, Liu G, Zeng L (2010) Lateral flow nucleic acid biosensor for Cu²⁺ detection in aqueous solution with high sensitivity and selectivity. *Chem Commun* 46(47):9043–9045. <https://doi.org/10.1039/c0cc02782k>
122. Chen J, Zhou X, Zeng L (2013) Enzyme-free strip biosensor for amplified detection of Pb²⁺ based on a catalytic DNA circuit. *Chem Commun* 49(10):984–986. <https://doi.org/10.1039/c2cc37598b>
123. Mazumdar D, Liu J, Lu G, Zhou J, Lu Y (2010) Easy-to-use dipstick tests for detection of lead in paints using non-cross-linked gold nanoparticle-DNAzyme conjugates. *Chem Commun* 46(9):1416–1418. <https://doi.org/10.1039/b917772h>
124. Shyu R-H, Shyu H-F, Liu H-W, Tang S-S (2002) Colloidal gold-based immunochromatographic assay for detection of ricin. *Toxicol* 40(3):255–258. [https://doi.org/10.1016/s0041-0101\(01\)00193-3](https://doi.org/10.1016/s0041-0101(01)00193-3)
125. Xu H, Mao X, Zeng Q, Wang S, Kawde AN, Liu G (2009) Aptamer-functionalized gold nanoparticles as probes in a dry-reagent strip biosensor for protein analysis. *Anal Chem* 81(2):669–675. <https://doi.org/10.1021/ac8020592>
126. Jauset-Rubio M, Svobodova M, Mairal T, McNeil C, Keegan N, El-Shahawi MS, Bashammakh AS, Alyoubi AO, O'Sullivan CK (2016) Aptamer lateral flow assays for ultrasensitive detection of beta-Conglutinin combining recombinase polymerase amplification and tailed primers. *Anal Chem* 88(21):10701–10709. <https://doi.org/10.1021/acs.analchem.6b03256>
127. Liu G, Mao X, Phillips JA, Xu H, Tan W, Zeng L (2009) Aptamer-nanoparticle strip biosensor for sensitive detection of cancer cells. *Anal Chem* 81(24):10013–10018. <https://doi.org/10.1021/ac901889s>
128. Wu W, Zhao S, Mao Y, Fang Z, Lu X, Zeng L (2015) A sensitive lateral flow biosensor for Escherichia coli O157:H7 detection based on aptamer mediated strand displacement amplification. *Anal Chim Acta* 861:62–68. <https://doi.org/10.1016/j.aca.2014.12.041>
129. Mudanyali O, Dimitrov S, Sikora U, Padmanabhan S, Navruz I, Ozcan A (2012) Integrated rapid-diagnostic-test reader platform on a cellphone. *Lab Chip* 12(15):2678–2686. <https://doi.org/10.1039/d2lc40235a>
130. You DJ, Park TS, Yoon JY (2013) Cell-phone-based measurement of TSH using Mie scatter optimized lateral flow assays. *Biosens Bioelectron* 40(1):180–185. <https://doi.org/10.1016/j.bios.2012.07.014>
131. Yang J-S, Shin J, Choi S, Jung H-I (2017) Smartphone diagnostics unit (SDU) for the assessment of human stress and inflammation level assisted by biomarker ink, fountain pen, and origami holder for strip biosensor. *Sensor Actuat B Chem* 241:80–84. <https://doi.org/10.1016/j.snb.2016.10.052>
132. Song C, Zhi A, Liu Q, Yang J, Jia G, Shervin J, Tang L, Hu X, Deng R, Xu C, Zhang G (2013) Rapid and sensitive detection of beta-agonists using a portable fluorescence biosensor based on fluorescent nanosilica and a lateral flow test strip. *Biosens Bioelectron* 50:62–65. <https://doi.org/10.1016/j.bios.2013.06.022>
133. Ozalp VC, Zeydanli US, Lunding A, Kavruk M, Oz MT, Eyidogan F, Olsen LF, Oktem HA (2013) Nanoparticle embedded enzymes for improved lateral flow sensors. *Analyst* 138(15):4255–4259. <https://doi.org/10.1039/c3an00733b>
134. Zangheri M, Di Nardo F, Anfossi L, Giovannoli C, Baggiani C, Roda A, Mirasoli M (2015) A multiplex chemiluminescent biosensor for type B-fumonisin and aflatoxin B1 quantitative detection in maize flour. *Analyst* 140(1):358–365. <https://doi.org/10.1039/c4an01613k>

135. Paterson AS, Raja B, Garvey G, Kolhatkar A, Hagstrom AE, Kourentzi K, Lee TR, Willson RC (2014) Persistent luminescence strontium aluminate nanoparticles as reporters in lateral flow assays. *Anal Chem* 86(19):9481–9488. <https://doi.org/10.1021/ac5012624>
136. Zhao Y, Zhou C, Wu R, Li L, Shen H, Li LS (2015) Preparation of multi-shell structured fluorescent composite nanoparticles for ultrasensitive human procalcitonin detection. *RSC Adv* 5(8):5988–5995. <https://doi.org/10.1039/c4ra13362e>
137. Wang L, Chen W, Ma W, Liu L, Ma W, Zhao Y, Zhu Y, Xu L, Kuang H, Xu C (2011) Fluorescent strip sensor for rapid determination of toxins. *Chem Commun* 47(5):1574–1576. <https://doi.org/10.1039/c0cc04032k>
138. Li S, Liu C, Han B, Luo J, Yin G (2017) An electrochemiluminescence aptasensor switch for aldibarb recognition via ruthenium complex-modified dendrimers on multiwalled carbon nanotubes. *Microchim Acta* 184(6):1669–1675. <https://doi.org/10.1007/s00604-017-2177-4>
139. Wang R, Zhang W, Wang P, Su X (2018) A paper-based competitive lateral flow immunoassay for multi beta-agonist residues by using a single monoclonal antibody labelled with red fluorescent nanoparticles. *Microchim Acta* 185(3):191. <https://doi.org/10.1007/s00604-018-2730-9>
140. Wang Y, Wang Y, Li D, Xu J, Ye C (2018) Detection of nucleic acids and elimination of carryover contamination by using loop-mediated isothermal amplification and antarctic thermal sensitive uracil-DNA-glycosylase in a lateral flow biosensor: application to the detection of *Streptococcus pneumoniae*. *Microchim Acta* 185(4):212. <https://doi.org/10.1007/s00604-018-2723-8>
141. Zhang J, Lv X, Feng W, Li X, Li K, Deng Y (2018) Aptamer-based fluorometric lateral flow assay for creatine kinase MB. *Microchim Acta* 185(8):364. <https://doi.org/10.1007/s00604-018-2905-4>
142. Zeng Y, Liang D, Zheng P, Peng T, Sun S, Mari GM, Jiang H (2019) Immunochromatographic fluorometric determination of clenbuterol with enhanced sensitivity. *Microchim Acta* 186(4):225. <https://doi.org/10.1007/s00604-019-3326-8>
143. Deng J, Yang M, Wu J, Zhang W, Jiang X (2018) A self-contained chemiluminescent lateral flow assay for point-of-care testing. *Anal Chem* 90(15):9132–9137. <https://doi.org/10.1021/acs.analchem.8b01543>
144. Zangheri M, Mirasoli M, Guardigli M, Di Nardo F, Anfossi L, Baggiani C, Simoni P, Benassai M, Roda A (2019) Chemiluminescence-based biosensor for monitoring astronauts' health status during space missions: results from the international Space Station. *Biosens Bioelectron* 129:260–268. <https://doi.org/10.1016/j.bios.2018.09.059>
145. Li X, Lu D, Sheng Z, Chen K, Guo X, Jin M, Han H (2012) A fast and sensitive immunoassay of avian influenza virus based on label-free quantum dot probe and lateral flow test strip. *Talanta* 100:1–6. <https://doi.org/10.1016/j.talanta.2012.08.041>
146. Wu F, Yuan H, Zhou C, Mao M, Liu Q, Shen H, Cen Y, Qin Z, Ma L, Song Li L (2016) Multiplexed detection of influenza a virus subtype H5 and H9 via quantum dot-based immunoassay. *Biosens Bioelectron* 77:464–470. <https://doi.org/10.1016/j.bios.2015.10.002>
147. Anfossi L, Di Nardo F, Cavalera S, Giovannoli C, Spano G, Speranskaya ES, Goryacheva IY, Baggiani C (2018) A lateral flow immunoassay for straightforward determination of fumonisin mycotoxins based on the quenching of the fluorescence of CdSe/ZnS quantum dots by gold and silver nanoparticles. *Microchim Acta* 185(2):94. <https://doi.org/10.1007/s00604-017-2642-0>
148. Wu J, Ma J, Wang H, Qin D, An L, Ma Y, Zheng Z, Hua X, Wang T, Wu X (2019) Rapid and visual detection of benzothiostrubin residue in strawberry using quantum dot-based lateral flow test strip. *Sensor Actuat B Chem* 283:222–229. <https://doi.org/10.1016/j.snb.2018.11.137>
149. Zangheri M, Cevenini L, Anfossi L, Baggiani C, Simoni P, Di Nardo F, Roda A (2015) A simple and compact smartphone accessory for quantitative chemiluminescence-based lateral flow immunoassay for salivary cortisol detection. *Biosens Bioelectron* 64:63–68. <https://doi.org/10.1016/j.bios.2014.08.048>
150. Yeo SJ, Choi K, Cuc BT, Hong NN, Bao DT, Ngoc NM, Le MQ, Hang Nle K, Thach NC, Mallik SK, Kim HS, Chong CK, Choi HS, Sung HW, Yu K, Park H (2016) Smartphone-Based fluorescent diagnostic system for highly pathogenic H5N1 viruses. *Theranostics* 6(2):231–242. <https://doi.org/10.7150/thno.14023>
151. Qin W, Wang K, Xiao K, Hou Y, Lu W, Xu H, Wo Y, Feng S, Cui D (2017) Carcinoembryonic antigen detection with "handing"-controlled fluorescence spectroscopy using a color matrix for point-of-care applications. *Biosens Bioelectron* 90:508–515. <https://doi.org/10.1016/j.bios.2016.10.052>
152. Magiati M, Sevastou A, Kalogianni DP (2018) A fluorometric lateral flow assay for visual detection of nucleic acids using a digital camera readout. *Microchim Acta* 185(6):1–9. <https://doi.org/10.1007/s00604-018-2856-9>
153. Rong Z, Wang Q, Sun N, Jia X, Wang K, Xiao R, Wang S (2019) Smartphone-based fluorescent lateral flow immunoassay platform for highly sensitive point-of-care detection of Zika virus nonstructural protein 1. *Anal Chim Acta* 1055:140–147. <https://doi.org/10.1016/j.aca.2018.12.043>
154. You M, Lin M, Gong Y, Wang S, Li A, Ji L, Zhao H, Ling K, Wen T, Huang Y, Gao D, Ma Q, Wang T, Ma A, Li X, Xu F (2017) Household fluorescent lateral flow strip platform for sensitive and quantitative prognosis of heart failure using dual-color Upconversion nanoparticles. *ACS Nano* 11(6):6261–6270. <https://doi.org/10.1021/acsnano.7b02466>
155. Cheng N, Song Y, Fu Q, Du D, Luo Y, Wang Y, Xu W, Lin Y (2018) Aptasensor based on fluorophore-quencher nano-pair and smartphone spectrum reader for on-site quantification of multi-pesticides. *Biosens Bioelectron* 117:75–83. <https://doi.org/10.1016/j.bios.2018.06.002>
156. Liu J, Ji D, Meng H, Zhang L, Wang J, Huang Z, Chen J, Li J, Li Z (2018) A portable fluorescence biosensor for rapid and sensitive glutathione detection by using quantum dots-based lateral flow test strip. *Sensors Actuators B Chem* 262:486–492. <https://doi.org/10.1016/j.snb.2018.02.040>
157. Wang X, Choi N, Cheng Z, Ko J, Chen L, Choo J (2017) Simultaneous detection of dual nucleic acids using a SERS-Based lateral flow assay biosensor. *Anal Chem* 89(2):1163–1169. <https://doi.org/10.1021/acs.analchem.6b03536>
158. Xiao M, Xie K, Dong X, Wang L, Huang C, Xu F, Xiao W, Jin M, Huang B, Tang Y (2019) Ultrasensitive detection of avian influenza a (H7N9) virus using surface-enhanced Raman scattering-based lateral flow immunoassay strips. *Anal Chim Acta* 1053:139–147. <https://doi.org/10.1016/j.aca.2018.11.056>
159. Tran V, Walkenfort B, Konig M, Salehi M, Schlucker S (2019) Rapid, quantitative, and ultrasensitive point-of-care testing: a portable SERS reader for lateral flow assays in clinical chemistry. *Angew Chem* 58(2):442–446. <https://doi.org/10.1002/anie.201810917>
160. Shi Q, Huang J, Sun Y, Deng R, Teng M, Li Q, Yang Y, Hu X, Zhang Z, Zhang G (2018) A SERS-based multiple immunonanoprobe for ultrasensitive detection of neomycin and quinolone antibiotics via a lateral flow assay. *Microchim Acta* 185(2):84. <https://doi.org/10.1007/s00604-017-2556-x>
161. Abbas A, Brimer A, Slocik JM, Tian L, Naik RR, Singamaneni S (2013) Multifunctional analytical platform on a paper strip: separation, preconcentration, and subattomolar detection. *Anal Chem* 85(8):3977–3983. <https://doi.org/10.1021/ac303567g>

162. Fu X, Cheng Z, Yu J, Choo P, Chen L, Choo J (2016) A SERS-based lateral flow assay biosensor for highly sensitive detection of HIV-1 DNA. *Biosens Bioelectron* 78:530–537. <https://doi.org/10.1016/j.bios.2015.11.099>
163. Hwang J, Lee S, Choo J (2016) Application of a SERS-based lateral flow immunoassay strip for the rapid and sensitive detection of staphylococcal enterotoxin B. *Nanoscale* 8(22):11418–11425. <https://doi.org/10.1039/c5nr07243c>
164. Choi S, Hwang J, Lee S, Lim DW, Joo H, Choo J (2017) Quantitative analysis of thyroid-stimulating hormone (TSH) using SERS-based lateral flow immunoassay. *Sensor Actuat B Chem* 240:358–364. <https://doi.org/10.1016/j.snb.2016.08.178>
165. Khlebtsov BN, Bratashov DN, Byzova NA, Dzantiev BB, Khlebtsov NG (2018) SERS-based lateral flow immunoassay of troponin I by using gap-enhanced Raman tags. *Nano Res* 12(2): 413–420. <https://doi.org/10.1007/s12274-018-2232-4>
166. Li X, Yang T, Song Y, Zhu J, Wang D, Li W (2019) Surface-enhanced Raman spectroscopy (SERS)-based immunochromatographic assay (ICA) for the simultaneous detection of two pyrethroid pesticides. *Sensor Actuat B-Chem* 283: 230–238. <https://doi.org/10.1016/j.snb.2018.11.112>
167. Li Y, Tang S, Zhang W, Cui X, Zhang Y, Jin Y, Zhang X, Chen Y (2019) A surface-enhanced Raman scattering-based lateral flow immunosensor for colistin in raw milk. *Sensor Actuat B-Chem* 282:703–711. <https://doi.org/10.1016/j.snb.2018.11.050>
168. Shen H, Xie K, Huang L, Wang L, Ye J, Xiao M, Ma L, Jia A, Tang Y (2019) A novel SERS-based lateral flow assay for differential diagnosis of wild-type pseudorabies virus and gE-deleted vaccine. *Sensor Actuat B Chem* 282:152–157. <https://doi.org/10.1016/j.snb.2018.11.065>
169. Wu Z (2019) Simultaneous detection of listeria monocytogenes and Salmonella typhimurium by a SERS-Based lateral flow Immunochromatographic assay. *Food Anal Methods* 12(5): 1086–1091. <https://doi.org/10.1007/s12161-019-01444-4>
170. Lin L-K, Stanciu LA (2018) Bisphenol a detection using gold nanostars in a SERS improved lateral flow immunochromatographic assay. *Sensor Actuat B Chem* 276: 222–229. <https://doi.org/10.1016/j.snb.2018.08.068>
171. Yang Y, Ozsoz M, Liu G (2017) Gold nanocage-based lateral flow immunoassay for immunoglobulin G. *Microchim Acta* 184(7): 2023–2029. <https://doi.org/10.1007/s00604-017-2176-5>
172. Zhang J, Yu Q, Qiu W, Li K, Qian L, Zhang X, Liu G (2019) Gold-platinum nanoflowers as a label and as an enzyme mimic for use in highly sensitive lateral flow immunoassays: application to detection of rabbit IgG. *Microchim Acta* 186(6):357. <https://doi.org/10.1007/s00604-019-3464-z>
173. Lu X, Mei T, Guo Q, Zhou W, Li X, Chen J, Zhou X, Sun N, Fang Z (2018) Improved performance of lateral flow immunoassays for alpha-fetoprotein and vanillin by using silica shell-stabilized gold nanoparticles. *Microchim Acta* 186(1):2. <https://doi.org/10.1007/s00604-018-3107-9>
174. Yang D, Ma J, Zhang Q, Li N, Yang J, Raju PA, Peng M, Luo Y, Hui W, Chen C, Cui Y (2013) Polyelectrolyte-coated gold magnetic nanoparticles for immunoassay development: toward point of care diagnostics for syphilis screening. *Anal Chem* 85(14): 6688–6695. <https://doi.org/10.1021/ac400517e>
175. Juntunen E, Myrskyläinen T, Salminen T, Soukka T, Pettersson K (2012) Performance of fluorescent europium(III) nanoparticles and colloidal gold reporters in lateral flow bioaffinity assay. *Anal Biochem* 428(1):31–38. <https://doi.org/10.1016/j.ab.2012.06.005>
176. Shukla S, Leem H, Kim M (2011) Development of a liposome-based immunochromatographic strip assay for the detection of Salmonella. *Anal Bioanal Chem* 401(8):2581–2590. <https://doi.org/10.1007/s00216-011-5327-2>
177. Mao X, Wang W, Du TE (2013) Dry-reagent nucleic acid biosensor based on blue dye doped latex beads and lateral flow strip. *Talanta* 114:248–253. <https://doi.org/10.1016/j.talanta.2013.04.044>
178. Kalogianni DP, Boutsika LM, Kouremenou PG, Christopoulos TK, Ioannou PC (2011) Carbon nano-strings as reporters in lateral flow devices for DNA sensing by hybridization. *Anal Bioanal Chem* 400(4):1145–1152. <https://doi.org/10.1007/s00216-011-4845-2>
179. Blazkova M, Rauch P, Fukal L (2010) Strip-based immunoassay for rapid detection of thiabendazole. *Biosens Bioelectron* 25(9): 2122–2128. <https://doi.org/10.1016/j.bios.2010.02.011>
180. Takalkar S, Baryeh K, Liu G (2017) Fluorescent carbon nanoparticle-based lateral flow biosensor for ultrasensitive detection of DNA. *Biosens Bioelectron* 98:147–154. <https://doi.org/10.1016/j.bios.2017.06.045>
181. Qiu W, Xu H, Takalkar S, Gurung AS, Liu B, Zheng Y, Guo Z, Baloda M, Baryeh K, Liu G (2015) Carbon nanotube-based lateral flow biosensor for sensitive and rapid detection of DNA sequence. *Biosens Bioelectron* 64:367–372. <https://doi.org/10.1016/j.bios.2014.09.028>
182. Rundstrom G, Jonsson A, Martensson O, Mendel-Hartvig I, Venge P (2006) Lateral flow immunoassay using europium (III) chelate microparticles and time-resolved fluorescence for eosinophils and neutrophils in whole Blood. *Clin Chem* 53(2):342–348. <https://doi.org/10.1373/clinchem.2006.074021>
183. Kang JH, Kwon DH, Chung TW, Kim YD, Lee HG, Kim JW, Choe IS, Kim KW, Lim JS, Song EY, Kim CH (2007) Development of a simple and rapid immunochromatographic strip test for diarrhea-causative porcine rotavirus in swine stool. *J Virol Methods* 146(1–2):74–79. <https://doi.org/10.1016/j.jviromet.2007.06.002>
184. Liu C, Jia Q, Yang C, Qiao R, Jing L, Wang L, Xu C, Gao M (2011) Lateral flow immunochromatographic assay for sensitive pesticide detection by using Fe₃O₄ nanoparticle aggregates as color reagents. *Anal Chem* 83(17):6778–6784. <https://doi.org/10.1021/ac201462d>
185. Hou Y, Wang K, Xiao K, Qin W, Lu W, Tao W, Cui D (2017) Smartphone-Based dual-modality imaging system for quantitative detection of color or fluorescent lateral flow Immunochromatographic strips. *Nanoscale Res Lett* 12(1):291. <https://doi.org/10.1186/s11671-017-2078-9>
186. Ruppert C, Phogat N, Laufer S, Kohl M, Deigner HP (2019) A smartphone readout system for gold nanoparticle-based lateral flow assays: application to monitoring of digoxigenin. *Microchim Acta* 186(2):119. <https://doi.org/10.1007/s00604-018-3195-6>
187. H-b L, X-j D, Zang Y-X, Li P, Wang S (2017) SERS-Based lateral flow strip biosensor for simultaneous detection of listeria monocytogenes and Salmonella enterica serotype Enteritidis. *J Agric Food Chem* 65(47):10290–10299. <https://doi.org/10.1021/acs.jafc.7b03957>

Publisher's note Springer Nature remains neutral with regard to jurisdictional claims in published maps and institutional affiliations.